

**CLASSIFICATION OF THE GLASERITE STRUCTURES
FAMILY BY MEANS OF GROUP THEORY**

**GRUP TEORİSİ İLE GLASERİT YAPILAR AİLESİNİN
SINIFLANDIRILMASI**



SERPİL ALBAY

ASSOC. PROF. DR. EMRE TAŞCI
Supervisor

Submitted to
Graduate School of Science and Engineering of Hacettepe University
as a Partial Fulfillment to the Requirements
for the Award of the Degree of Master of Science
in Physics Engineering.

2019

This work titled "**Classification of The Glaserite Structures Family by means of Group Theory**" by **Serpil Albay** has been approved as a thesis for the Degree of **Master of Science in Physics Engineering** by the Examining Committee Members mentioned below.

Prof. Dr. Süheyla Özbey

Head



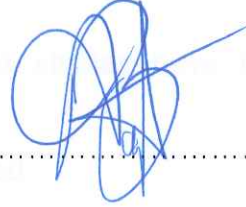
Assoc. Prof. Dr. Emre Taşçı

Supervisor



Assoc. Prof. Dr. Akın Bacioğlu

Member



Assoc. Prof. Dr. Emine Deniz Tekin

Member



Assist. Prof. Dr. Osman Barış Malcıoğlu

Member



This thesis has been approved as a thesis for the Degree of **Master of Science in Physics Engineering** by Board of Directors of the Institute of Graduate School of Science and Engineering on / /.....

Prof. Dr. Menemşe GÜMÜŞDERELİOĞLU

Director of the Institute of

Graduate School of Science and Engineering

ETHICS

In this thesis study, prepared in accordance with the spelling rules of Institute of Graduate School of Science and Engineering of Hacettepe University,

I declare that

- all the information and documents have been obtained in the base of the academic rules
- all audio-visual and written information and results have been presented according to the rules of scientific ethics
- in case of using other works, related studies have been cited in accordance with the scientific standards
- all cited studies have been fully referenced
- I did not do any distortion in the data set
- and any part of this thesis has not been presented as another thesis study at this or any other university.

.14. / .06 / 2019



Serpil Albay

YAYIMLANMA FİKRİ MÜLKİYET HAKLARI BEYANI

Enstitü tarafından onaylanan lisansüstü tezimin/raporumun tamamını veya herhangi bir kısmını, basılı (kağıt) ve elektronik formatta arşivleme ve aşağıda verilen koşullarla kullanıma açma iznini Hacettepe üniversitesine verdiğimi bildiririm. Bu izinle Üniversiteye verilen kullanım hakları dışındaki tüm fikri mülkiyet haklarım bende kalacak, tezimin tamamının ya da bir bölümünün gelecekteki çalışmalarda (makale, kitap, lisans ve patent vb.) kullanım hakları bana ait olacaktır.

Tezin kendi orijinal çalışmam olduğunu, başkalarının haklarını ihlal etmediğimi ve tezimin tek yetkili sahibi olduğumu beyan ve taahhüt ederim. Tezimde yer alan telif hakkı bulunan ve sahiplerinden yazılı izin alınarak kullanması zorunlu metinlerin yazılı izin alarak kullandığımı ve istenildiğinde suretlerini Üniversiteye teslim etmeyi taahhüt ederim.

Yükseköğretim Kurulu tarafından yayınlanan "**Lisansüstü Tezlerin Elektronik Ortamda Toplanması, Düzenlenmesi ve Erişime Açılmasına İlişkin Yönerge**" kapsamında tezim aşağıda belirtilen koşullar haricince YÖK Ulusal Tez Merkezi / H. Ü. Kütüphaneleri Açık Erişim Sisteminde erişime açılır.

- Enstitü / Fakülte yönetim kurulu kararı ile tezimin erişime açılması mezuniyet tarihimden itibaren 2 yıl ertelenmiştir.
- Enstitü / Fakülte yönetim kurulu gerekçeli kararı ile tezimin erişime açılması mezuniyet tarihimden itibaren ay ertelenmiştir.
- Tezim ile ilgili gizlilik kararı verilmiştir.

14. / 06 / 2019



Serpil Albay

ABSTRACT

CLASSIFICATION OF THE GLASERITE STRUCTURES FAMILY BY MEANS OF GROUP THEORY

Serpil Albay

Master of Science, Department of Physics Engineering

Supervisor: Assoc. Prof. Dr. Emre Taşcı

June 2019, 91 pages

In this thesis, an extensive analysis of the evaluation of group-subgroup relations of glaserite-type compounds by means of group theory phase transition constraints is aimed. Relations of more than 100 structures were used to create a diagram tree containing the information of structures, index, transformation matrix, lattice distortion and global distortion, as well as possible theoretical structures evaluated in order to find intermediate glaserite-type compounds between the high and low symmetry structures. Glaserite-type compounds are compared among the most related structures according to their cation occupancies of their general chemical formula. Comparison of the crystals was obtained in accordance with their symmetry information via Bilbao Crystallographic Server online tools. In addition, the case study was demonstrated step by step to calculate and analyze the group-subgroup relations of $\text{BaNa}(\text{PO}_4)_2$ crystal via transformation of $P-3m1$ minimal supergroup to $C2/m$ maximal subgroup.

Keywords: Glaserite, Glaserite-type structure, crystallography, group-subgroup relations, symmetry

ÖZET

GRUP TEORİSİ İLE GLASERİT YAPILAR AİLESİNİN SINIFLANDIRILMASI

Serpil Albay

Yüksek Lisans, Fizik Mühendisliği Bölümü

Danışman: Doç. Dr. Emre Taşcı

Haziran 2019, 91 sayfa

Bu tez çalışmasında, glaserite-tipi yapıların, grup teorisinin izin verdiği grup-altgrup geçişlerinin kapsamlı bir şekilde değerlendirilmesi amaçlanmıştır. 100'den fazla glaserite-tipi bileşik kullanılarak diyagram oluşturulmuştur. Bu diyagramda, yapı bilgisi, indis, dönüşüm matrisi, örgü ve genel bozulma bilgileri yer almaktadır. Bu bilgilerin yanı sıra, yüksek ve düşük simetri yapıları arasında bulunan olası ara bileşikler de öngörülerek diyagrama eklenmiştir. Glaserit- tipi yapıların kimyasal formülündeki katyon doluluğuna göre, yapısal olarak birbirine en yakın olanlar arasında karşılaştırma yapılmıştır. Kristal yapılar, uzay gruplarına göre, Bilbao Kristalografi sunucusunun çevrimiçi araçları kullanılarak karşılaştırılmıştır. Bunun yanı sıra, $\text{BaNa}(\text{PO}_4)_2$ kristalinin $P - 3m1$ (#164) uzay grubundan $C2/m$ (#12) uzay grubuna geçişi örnek incelemesi olarak detaylıca ele alınmıştır.

Anahtar Kelimeler: Glaserite, Glaserite-tipi yapılar, kristalografi, grup-altgrup ilişkileri, simetri

ACKNOWLEDGEMENT

First and foremost, I would like to thank my supervisor Assoc. Prof. Dr. Emre Taşcı for his guidance and support. He has always been helpful, full of kindness, patient, and ready to share his knowledge and he also supported me whenever I fall into trouble. He, beyond a supervisor, provided an opportunity for me when I felt hopeless so that I could write my thesis thanks to him. I learned not only academic knowledge but also being kind and optimistic person from him. I see him an inspiring role model as everyone does who meets him. I am always grateful for being his student.

I would also like to thank my sister Sibel Albay and my friends Delal Şeker, Alper Özkök and Şeyma Torgutalp for their supportive manners, continuous encouragement and helps throughout writing this thesis.

Special thanks to Delal Şeker for her time she had spent devotedly with me while writing this thesis and for taking flower photographs to see examples of symmetrical figures in nature.

I thank Rosica Nikolova & Vlad Kostov-Kytin for generously sharing the glaserite-type structures' data that they have collected.

This thesis has been supported by Hacettepe University Research Funds (Project No: FDS-2015-6628).

CONTENTS

ABSTRACT	i
ÖZET	ii
ACKNOWLEDGEMENT	iii
CONTENTS	iv
LIST OF TABLES	vii
LIST OF FIGURES	viii
ABBREVIATIONS AND SYMBOLS	x
I. GROUP THEORY	1
1. SYMMETRY	1
1.1. Isometries – Symmetry Operations	1
1.2. Graphical Representation	2
1.3. Matrix-Column Representation	4
1.4. Augmented Matrix	7
1.5. Seitz Notation	9
2. GROUP AXIOMS	12
3. GROUP RELATIONS	14
3.1. Group-Subgroup Relations	14
3.2. Index	15
3.3. Conjugacy Class	16
3.4. Conjugate Subgroups	17
3.5. Normalizers	18
3.6. Coset Decomposition	19
3.7. Transformation Matrix	20

3.8.	Metric Tensor	23
II.	GROUP THEORY IN SOLID STATE PHYSICS	25
4.	POINT GROUPS	25
5.	BRAVAIS LATTICES	27
5.1.	Triclinic.....	28
5.2.	Monoclinic.....	28
5.3.	Orthorhombic	28
5.4.	Tetragonal.....	29
5.5.	Hexagonal.....	29
5.6.	Trigonal (Rhombohedral)	29
5.7.	Cubic.....	29
5.8.	Unit Cell, Primitive Cell, Centring Factor	30
5.9.	Pearson Symbol.....	31
6.	SPACE GROUP	33
6.1.	Hermann-Mauguin Notation	33
6.2.	Classification of Symmetry Operations	35
6.2.1.	Identity	36
6.2.2.	Translation.....	36
6.2.3.	Rotation or Screw Rotation.....	36
6.2.4.	Inversion	36
6.2.5.	Rotoinversion.....	36
6.2.6.	Reflection or Glide Reflection	37
6.3.	Site symmetry	37
6.4.	Wyckoff Position.....	37
6.4.1.	General Position vs Special Positions	38
6.5.	Description of Structures.....	40
7.	GROUP- SUBGROUP RELATIONS.....	42

7.1.	Index.....	42
7.1.1.	Translationengleiche Index (i_p).....	42
7.1.2.	Klassengleiche Index (i_i).....	43
7.2.	Transformation Matrix.....	43
7.3.	Wyckoff Position Splitting	44
7.4.	Spontaneous Strain	44
7.5.	Bärnighausen Tree	45
7.6.	Case Study	46
III.	APPLICATION OF GROUP THEORY TO THE GLASERITE-TYPE STRUCTURES FAMILY	68
8.	INTRODUCTION TO GLASERITE AND GLASERITE-TYPE COMPOUNDS	68
9.	CLASSIFICATION OF KNOWN GLASERITE-TYPE COMPOUNDS	71
10.	IDENTIFICATION OF RELATIONS OF GLASERITE-TYPE SUB-FAMILIES	74
11.	CONCLUSION	82
	REFERENCES	85
	THESIS ORIGINALITY REPORT	89
	CURRICULUM VITAE	90

LIST OF TABLES

Table 1.1. Multiplication Table (also known as Cayley Table).....	3
Table 1.2. Seitz Notation of the General Position of $P3_2$	9
Table 4.1. Three Dimensional Crystal Systems and Point Groups	25
Table 5.1. Crystal Systems and Bravais Lattices	27
Table 5.2. Unit Cell Centring	30
Table 5.3. Pearson Symbols of Bravais Lattices	31
Table 6.1. Space Groups with Corresponding Crystal System Numbers	33
Table 6.2. Principal Directions of the Point Groups	34
Table 6.3 Characterization of the Matrix W	35
Table 7.1. Wyckoff Positions of $P-3m1$	53
Table 7.2. Wyckoff Positions of $C2/m$	53
Table 7.3. Wyckoff Splitting Compatibility	55
Table 7.4. Atomic Positions and Wyckoff Positions of $BaNa(PO_4)_2$ (#164)	61
Table 7.5. Atomic Positions and Wyckoff Positions of $BaNa(PO_4)_2$ (#12)	63
Table 9.1. Derivatives of the General Formula of GTC	72
Table 10.1. Relations of Glaserite-type Sub-Families	75

LIST OF FIGURES

Figure 1.1. Order of 4 + Operation	2
Figure 3.1 Related Groups and Subgroups	15
Figure 3.2 Subgroup Chain.....	16
Figure 3.3 Origin Shift.....	21
Figure 3.4 Change of Basis	23
Figure 3.5 Intervector Angles in 3D	24
Figure 6.1 Wyckoff Sets of Space Group $C2/m$	38
Figure 6.2. Unit Cell Representation of $P - 3m1$ Space Group and its Symmetry Operations	39
Figure 6.3. General Position and Special Positions of $P - 3m1$	40
Figure 6.4. Description of a Structure	41
Figure 7.1. Bärnighausen Tree Representing Group-Subgroup Relation	45
Figure 7.2. $BaNa(PO_4)_2$ ($P-3m1$) (#164) Parameters.....	46
Figure 7.3. $BaNa(PO_4)_2$ ($P-3m1$) Structure	46
Figure 7.4. $BaNa(PO_4)_2$ ($C2/m$) (#12) Parameters.....	47
Figure 7.5. $BaNa(PO_4)_2$ ($C2/m$) Structure	47
Figure 7.6. Conjugated maximal subgroups of the minimal supergroup	51
Figure 7.7. Transformation of the Wyckoff Positions of ($C2/m$) via Elements of Euclidean Normalizer.....	54
Figure 7.8. Reference Structure vs. Glaserite-type Structure of $C2/m$ Space Group.....	56

Figure 7.9. General Formula of Affine Normalizer of $C2/m$ Space Group (unique axis b) (u:odd; n:integer; g:even).....	57
Figure 7.10. Identical Transformation Matrices between the Group and the Subgroups.....	58
Figure 7.11. Symmetry Operators of $C2/m$	62
Figure 7.12. Atomic Displacements between Reference Structure and Glaserite-type Structure.....	67
Figure 8.1. Hexagonal Packing Composed of Two Types of Columns	69
Figure 8.2. Hexagonal Arrangement of the Glaserite	69

ABBREVIATIONS AND SYMBOLS

Abbreviations

GTC	Glaserite-type compound
GTS	Glaserite-type structure
GTT	Glaserite-type topology
SR	Structure relations

Symbols

i_p	Translationengleiche index
i_l	Klassengleiche index
i	Total index
G	Metric tensor
(P, p)	Transformation matrix pair
(W, w)	Matrix-column pair
W	Affine mappings
\mathbf{W}	Augmented matrix
S	Strain
Z	Number of conventional formula unit
f	Centring factor
N_E	Euclidean normalizer
N_A	Affine normalizer
$a, b, c, \alpha, \beta, \gamma$	Lattice parameters

I. GROUP THEORY

1. SYMMETRY

Symmetry deals with similarity between the portions of an object or a living being. In nature, there are a lot of examples of symmetry that show symmetrical pattern like butterfly wings, honeycombs, starfishes, flowers, snowflake, etc. The beauty of the nature originates from the sense of the symmetry. Generally, symmetry provides advantages for animals and, flowers through every part of the nature. Advantages might manifest themselves in the hunt for a cheetah who needs to run quickly, or might be a flap for a bird, or might be the pollination for a flower which needs to seem attractive. However, asymmetry is sometimes also a way to survive with respect to requirements of adaptation. Rotational symmetry, mirror symmetry, translational symmetry and reflection are some of the symmetry types existed in two and three dimensions [1].

1.1. Isometries – Symmetry Operations

Isometric mapping maintains all distances and angles unchanged while affine mappings do not maintain distances invariant but preserve parallelism. Parallel shift is called translation [2]. Isometries are special form of affine mappings and they do not let any distortion between the image of a body and the original body [3]. Since there is no distortion, the image of a body has the same volume with the main body. So, this stability of the volume can be expressed by the following condition:

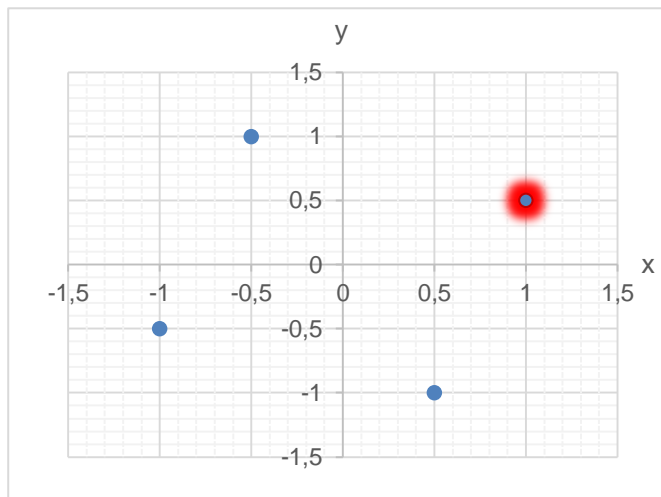
$$\det(W) = \pm 1$$

Where W is an isometry represented in matrix-column representation of the mapping (discussed in Section 1.3).

Symmetry denotes infinite integration of parts by which isometries map onto a whole object. Mapping onto itself means that an observer cannot realize the difference of the object's state between before and after the mapping [3].

1.2. Graphical Representation

An easy way of understanding the repeating order is to choose a point in two dimensional coordinate system. For example, the point at (1,0.5) can be rotated counter-clockwise direction by an angle of 90° four times to coincide with its initial point.



$$4^+ \begin{pmatrix} 1 \\ 0.5 \end{pmatrix} = \begin{pmatrix} -0.5 \\ 1 \end{pmatrix}$$

$$4^+ \begin{pmatrix} -0.5 \\ 1 \end{pmatrix} = \begin{pmatrix} -1 \\ -0.5 \end{pmatrix}$$

$$4^+ \begin{pmatrix} -1 \\ -0.5 \end{pmatrix} = \begin{pmatrix} 0.5 \\ -1 \end{pmatrix}$$

$$4^+ \begin{pmatrix} 0.5 \\ -1 \end{pmatrix} = \begin{pmatrix} 1 \\ 0.5 \end{pmatrix}$$

Figure 1.1. Order of 4^+ Operation

$$1. \quad 4^+ \begin{pmatrix} x \\ y \end{pmatrix} = \begin{pmatrix} -y \\ x \end{pmatrix}$$

$$3. \quad 4^+ \begin{pmatrix} -x \\ -y \end{pmatrix} = \begin{pmatrix} y \\ -x \end{pmatrix}$$

$$2. \quad 4^+ \begin{pmatrix} -y \\ x \end{pmatrix} = \begin{pmatrix} -x \\ -y \end{pmatrix}$$

$$4. \quad 4^+ \begin{pmatrix} y \\ -x \end{pmatrix} = \begin{pmatrix} x \\ y \end{pmatrix}$$

If we select our initial point as (1, 0) and (0, 1), we can easily write 4^+ operation in general form by examining its effect on these points.

$$4^+ \begin{pmatrix} 1 \\ 0 \end{pmatrix} = \begin{pmatrix} 0 \\ 1 \end{pmatrix}$$

$$4^+ \begin{pmatrix} 0 \\ 1 \end{pmatrix} = \begin{pmatrix} -1 \\ 0 \end{pmatrix}$$

Then, general matrix representation of fourfold symmetry operator in two dimensions becomes;

$$4^+ = \begin{pmatrix} 0 & -1 \\ 1 & 0 \end{pmatrix}$$

Applying 4^+ operation only a finite number of times is not sufficient to explore the full symmetry (that is, before reaching the identity operation) since symmetry has a meaning only when it is applied repeatedly until no new components can be derived.

Table 1.1. Multiplication Table (also known as Cayley Table)

	I	4⁺	2	4⁻
I	I	4 ⁺	2	4 ⁻
4⁺	4 ⁺	2	4 ⁻	I
2	2	4 ⁻	I	4 ⁺
4⁻	4 ⁻	I	4 ⁺	2

In Table 1.1, operation 4^+ shows counter-clockwise rotation of 90° , 4^- shows clockwise rotation of 90° and I is identity. 2 represents a rotation of 180° and thus, choosing direction of rotation makes no difference.

General formula of rotation axis in 2-dimensional coordinate system is defined as [4];

$$R = \begin{pmatrix} \cos(2\pi/n) & -\sin(2\pi/n) \\ \sin(2\pi/n) & \cos(2\pi/n) \end{pmatrix}$$

n shows number of rotations needed to overlap final point and initial point.

In 3-dimensional system, rotation axis specifies the rotation matrices. Rotations about the x , y and z axes are defined as [4];

$$R_x(2\pi/n) = \begin{pmatrix} 1 & 0 & 0 \\ 0 & \cos(2\pi/n) & -\sin(2\pi/n) \\ 0 & \sin(2\pi/n) & \cos(2\pi/n) \end{pmatrix}$$

$$R_y(2\pi/n) = \begin{pmatrix} \cos(2\pi/n) & 0 & -\sin(2\pi/n) \\ 0 & 1 & 0 \\ \sin(2\pi/n) & 0 & \cos(2\pi/n) \end{pmatrix}$$

$$R_z(2\pi/n) = \begin{pmatrix} \cos(2\pi/n) & -\sin(2\pi/n) & 0 \\ \sin(2\pi/n) & \cos(2\pi/n) & 0 \\ 0 & 0 & 1 \end{pmatrix}$$

Example: Consider 3 dimensional coordinate system. Let's write 2-fold rotational symmetry matrix along x axis.

$$R_x(\pi) = \begin{pmatrix} 1 & 0 & 0 \\ 0 & \cos(\pi) & -\sin(\pi) \\ 0 & \sin(\pi) & \cos(\pi) \end{pmatrix}$$

$$\mathbf{2} = \begin{pmatrix} 1 & 0 & 0 \\ 0 & -1 & 0 \\ 0 & 0 & -1 \end{pmatrix}$$

Symmetry operation found above $(x, -y, -z)$ (to be read in row-wise direction with $x[1 \ 0 \ 0], y[0 \ -1 \ 0], z[0 \ 0 \ -1]$) is representative matrix showing a rotation about x -axis by choosing coordinate system (x, y, z) . If different coordinate system is chosen, not the 2-fold rotational symmetry operation itself but its representation is changed according to new coordinates.

Since a symmetry operation maps a position to another, it is equivalent to an active transformation and if need arises, it can also be interpreted as a passive transformation where the coordinate system (i.e., the axes) is manipulated to yield the same result.

1.3. Matrix-Column Representation

Affine mappings W can be described using a coordinate system that is referred by a system of linear equations. A (3×3) matrix W and a (3×1) column vector w constitute the matrix-column pair (W, w) .

Thus, a general position (x'_1, x'_2, x'_3) related to another position (x_1, x_2, x_3) via an affine mapping (W, w) can be expressed as:

$$\begin{aligned}x'_1 &= W_{11}x_1 + W_{12}x_2 + W_{13}x_3 + w_1 \\x'_2 &= W_{21}x_1 + W_{22}x_2 + W_{23}x_3 + w_2 \\x'_3 &= W_{31}x_1 + W_{32}x_2 + W_{33}x_3 + w_3\end{aligned}$$

In matrix form:

$$\begin{pmatrix} x'_1 \\ x'_2 \\ x'_3 \end{pmatrix} = \begin{pmatrix} W_{11} & W_{12} & W_{13} \\ W_{21} & W_{22} & W_{23} \\ W_{31} & W_{32} & W_{33} \end{pmatrix} \begin{pmatrix} x_1 \\ x_2 \\ x_3 \end{pmatrix} + \begin{pmatrix} w_1 \\ w_2 \\ w_3 \end{pmatrix}$$

This may be abbreviated as:

$$x' = Wx + w = (W, w)x$$

Composition of the two mappings W_1 and W_2 produce a new affine mapping W_3 as follows:

$$W_3 = W_2W_1$$

Here, the order of operations is important as in general they do not commute.

$$W_2W_1 \neq W_1W_2$$

Rule of composition can be obtained by successively acting the (W_1, w_1) and (W_2, w_2) operator pairs on a position x .

$$\begin{aligned}x' &= W_1x + w_1 \\x'' &= W_2x' + w_2 = W_2W_1x + W_2w_1 + w_2\end{aligned}$$

If $x'' = W_3x + w_3$, then (W_3, w_3) pair equals to the following equation that shows successive application of W_1 and W_2 mappings.

$$(W_3, w_3) = (W_2 W_1, W_2 w_1 + w_2)$$

Each affine mapping pair is a combination of the (I, w) and $(W, 0)$. The mappings pair with unit matrix, (I, w) , represents translations and $(W, 0)$ describes rotational part and keeps origin fixed. Consequently, W characterizes the linear part while w represents the translational part of the affine mapping W [2].

Inverse affine mapping occurs on the condition that $\det(W) \neq 0$. For the (W, w) pair, the following equations can be derived:

$$(W, w)^{-1}(W, w) = (I, 0)$$

$$(W^{-1}W, W^{-1}w - W^{-1}w) = (I, 0)$$

$$\text{Thus, } (W, w)^{-1} = (W^{-1}, -W^{-1}w)$$

$$\text{If } x' = Wx + w, \text{ then, } x = W^{-1}x' - W^{-1}w$$

Isometries cannot be defined with only using (3×3) W matrices since the distances are preserved. Isometries always obey the condition $\det(W) = \pm 1$ and they are always invertible. Successive and inverse products $(W_2 W_1$ and $W^{-1})$ of affine mapping pairs are also included in the set of all isometries that forms a group [2].

We can proceed with an example to show affine mapping pairs and isometry conditions.

Example: Consider the representation of the 3_2 threefold screw rotation axis:

$$-y, x - y, z + 2/3$$

Linear equations refer to the coordinate system describing affine mappings:

$$x'_1 = -y$$

$$x'_2 = x - y$$

$$x'_3 = z + 2/3$$

Case of $x' = x$ shows that x is a fixed point that is invariant under this mapping. But in this example there is no fixed point since the motion is the screw rotation. Linear and translation parts will be represented as follows in matrix form:

$$W = \begin{pmatrix} 0 & -1 & 0 \\ 1 & -1 & 0 \\ 0 & 0 & 1 \end{pmatrix} \text{ and } w = \begin{pmatrix} 0 \\ 0 \\ 2/3 \end{pmatrix}$$

$$\begin{pmatrix} x'_1 \\ x'_2 \\ x'_3 \end{pmatrix} = \begin{pmatrix} 0 & -1 & 0 \\ 1 & -1 & 0 \\ 0 & 0 & 1 \end{pmatrix} \begin{pmatrix} x \\ y \\ z \end{pmatrix} + \begin{pmatrix} 0 \\ 0 \\ 2/3 \end{pmatrix}$$

$$\det \begin{vmatrix} 0 & -1 & 0 \\ 1 & -1 & 0 \\ 0 & 0 & 1 \end{vmatrix} = 1, \text{ satisfies the } \det(W) = \pm 1 \text{ condition.}$$

(W, w) pair can be written in (3×4) matrix form. In order to check the invertibility condition, we have to convert the pair into a (4×4) augmented matrix form which is defined in Section 1.4

$$\mathbf{W} = \left(\begin{array}{ccc|c} 0 & -1 & 0 & 0 \\ 1 & -1 & 0 & 0 \\ 0 & 0 & 1 & 2/3 \\ \hline 0 & 0 & 0 & 1 \end{array} \right)$$

$$\mathbf{W}^{-1} = \left(\begin{array}{ccc|c} -1 & 1 & 0 & 0 \\ -1 & 0 & 0 & 0 \\ 0 & 0 & 1 & -2/3 \\ \hline 0 & 0 & 0 & 1 \end{array} \right) \text{ and } \mathbf{W}^{-1} \times \mathbf{W} = \left(\begin{array}{ccc|c} 1 & 0 & 0 & 0 \\ 0 & 1 & 0 & 0 \\ 0 & 0 & 1 & 0 \\ \hline 0 & 0 & 0 & 1 \end{array} \right) = (I, 0)$$

1.4. Augmented Matrix

The system of equations is a combination of a (3×3) matrix W and (3×1) column-vector w in a (3×4) matrix. In order to avoid complications, it is

possible to add a 4th row (0 0 0 1) to the system equation to complete it to a square matrix. This re-formed square matrix is called the *augmented matrix* [2].

$$\mathbf{W} = \left(\begin{array}{ccc|c} & & & w \\ & W & & \\ \hline 0 & 0 & 0 & 1 \end{array} \right)$$

An affine mapping pair (W, w) can be described now in augmented form \mathbf{W} . Successive application of the pairs is defined as the multiplication of their augmented matrices.

$$\mathbf{W}_3 = \mathbf{W}_2 \mathbf{W}_1$$

Thus, inverse affine mapping can also be represented by \mathbf{W}^{-1} as an alternative form to $(W, w)^{-1} = (W^{-1}, -W^{-1}w)$. Similar to column w , x' and x have to be augmented to (4×1) matrices. Determinant of the linear part (or rotational part) W and augmented matrix \mathbf{W} are equal.

```
>> W1=[0 -1 0;1 -1 0;0 0 1]
W1 =
```

```
0 -1 0
1 -1 0
0 0 1
```

```
>> W2=[0 -1 0 0;1 -1 0 0;0 0 1 2/3;0 0 0 1]
W2 =
```

```
0.00000 -1.00000 0.00000 0.00000
1.00000 -1.00000 0.00000 0.00000
0.00000 0.00000 1.00000 0.66667
0.00000 0.00000 0.00000 1.00000
```

$\det(W) = \det(\mathbf{W}) \quad \checkmark$

```
>> det(W1)
ans = 1
>> det(W2)
ans = 1
```

$$\det(W) = \det(\mathbf{W}) = 1$$

$$\det \begin{vmatrix} 0 & -1 & 0 \\ 1 & -1 & 0 \\ 0 & 0 & 1 \end{vmatrix} = \det \begin{vmatrix} 0 & -1 & 0 & 0 \\ 1 & -1 & 0 & 0 \\ 0 & 0 & 1 & 2/3 \\ 0 & 0 & 0 & 1 \end{vmatrix} = 1$$

1.5. Seitz Notation

Seitz symbol is a notation that describes the symmetry operations of the space groups. Seitz symbols consist of a rotation part R and a translation part t .

$$\{ R | t \}$$

Corresponding symbols to R shows the type of the symmetry and orientation of the symmetry elements to the basis. [5]

Symbols of R :

- 1 is used for the identity
- -1 is used for the inversion
- m is used for reflections
- 2, 3, 4 and 6 for rotations
- -3 , -4 , and -6 are used for rotoinversions

Example: General position of $P3_2$ (#145) has the following coordinate triplets and corresponding Seitz symbols:

Table 1.2. Seitz Notation of the General Position of $P3_2$

Coordinate Triplets	ITA Symbol	Seitz Symbol
x, y, z	1	$\{ 1 0 \}$
$-y, x - y, z + 2/3$	$3^+(0, 0, 2/3) 0 0 z$	$\{ 3_{001}^+ 0 0 2/3 \}$
$-x + y, -x, z + 1/3$	$3^-(0, 0, 1/3) 0 0 z$	$\{ 3_{001}^- 0 0 1/3 \}$

Superscript signs (+/−) show direction of rotation. While “ − ” sign indicates clockwise rotations, “ + ” sign points to counter-clockwise rotations. Subscript of the rotation part shows characteristic direction of motion by indicating the rotation around an axis. In the view of such information, for the operation denoted by $\{ 3_{001}^+ | 0 0 2/3 \}$ symbol, we can explain that there is a rotation by 120° angle around z axis followed by a translation by $2/3$ along z axis.

Example: Let's choose a point with the coordinates (0.2 0.3 0.4)

$$\begin{pmatrix} x \\ y \\ z \end{pmatrix} = \begin{pmatrix} 0.2 \\ 0.3 \\ 0.4 \end{pmatrix}$$

Then, we apply left-handed 3_2 screw rotation operation $\{ 3_{001}^+ | 0 0 2/3 \}$:

$$\begin{pmatrix} x'_1 \\ x'_2 \\ x'_3 \end{pmatrix} = \begin{pmatrix} 0 & -1 & 0 \\ 1 & -1 & 0 \\ 0 & 0 & 1 \end{pmatrix} \begin{pmatrix} 0.2 \\ 0.3 \\ 0.4 \end{pmatrix} + \begin{pmatrix} 0 \\ 0 \\ 2/3 \end{pmatrix}$$

After the first rotation by 120° and translation along z, the new coordinate of the point will be:

$$\begin{pmatrix} x'_1 \\ x'_2 \\ x'_3 \end{pmatrix} = \begin{pmatrix} -0.3 \\ -0.1 \\ 16/15 \end{pmatrix}$$

After the second consecutive application of the operation:

$$\begin{pmatrix} x'_1 \\ x'_2 \\ x'_3 \end{pmatrix} = \begin{pmatrix} 0.1 \\ -0.2 \\ 26/15 \end{pmatrix}$$

And after applying the operation for a third time, the point comes to its initial coordinates on x and y axes.

There is translation only along z axis. So, if one looks the point over z axis, the initial point seems not to change at all (and by employing crystallographic unit cell translations, this point can be shown to be equivalent to the starting point as $12/5 \rightarrow 2/5 = 0.4$).

$$\begin{pmatrix} x'_1 \\ x'_2 \\ x'_3 \end{pmatrix} = \begin{pmatrix} 0.2 \\ 0.3 \\ 12/5 \end{pmatrix} = \begin{pmatrix} 1 & 0 & 0 \\ 0 & 1 & 0 \\ 0 & 0 & 6 \end{pmatrix} \begin{pmatrix} 0.2 \\ 0.3 \\ 0.4 \end{pmatrix}$$



2. GROUP AXIOMS

The set of isometries correspond to a symmetry group if it satisfies the following 4 axioms [2]:

Let G be a set of isometries (symmetry group).

1- Identity

A group has a special symmetry element I such that upon being operated on another element of the group the result is the operated element itself. This I element is called the *identity element* of the group.

g_i is an element of G

I such that $Ig_i = g_iI = g_i, \forall g_i \in G$

2- Invertibility

For each symmetry element g of the group, there is a corresponding element g^{-1} such that upon being operated on each other the result is the identity operator I , and g^{-1} is called the *inverse of g* operator.

g^{-1} is inverse of g

g such that $g^{-1}g = gg^{-1} = I, \forall g, g^{-1} \in G$

3- Associativity

For three elements g_i, g_j, g_k of the group, as long as the order of the elements is kept, any order of operations yields the same result.

$g_i(g_jg_k) = (g_ig_j)g_k, \forall g_i, g_j, g_k \in G$

4- Closure

If g_i, g_j are elements of the group, their product g_k must also be an element of the group.

$g_i, g_j \in G$ and $g_ig_j = g_k$, then $g_k \in G$

Some Definitions [2]:

- If $g_i g_j = g_j g_i$ for all pairs in G , group is called Abelian (commutative).
- If all elements of a group can be obtained by one of its elements, the group is called cyclic.

$$\text{e.g. } G = \{g_i, g_i^2, g_i^3, \dots\}$$

- If G is an Abelian group and $g_i^n = I$, then group G is called finite and cyclic of order n .

3. GROUP RELATIONS

3.1. Group-Subgroup Relations

Relationship between symmetries points out correlation of group and subgroup. Group-subgroup relation plays a significant role the comparison of crystal structures.

Symmetry group consists of its symmetry operations and these operations must obey closure, identity, associativity and invertibility rules as explained in the previous section.

Let G and H represent two symmetry groups;

$$G = \{g_1, g_2, g_3, g_4, \dots, g_i\} \quad \text{and} \quad H = \{h_1, h_2, h_3, h_4, \dots, h_j\}$$

If each $h_i \in G$, then H is a subgroup of G and G is a supergroup of H and thus denoted by the symbol:

$$H < G$$

If there is no intermediate group between G and H , then H is a *maximal subgroup* of G , and G is a *minimal supergroup* of H .

If we have two symmetry groups and there is a group-subgroup relation between them, expressing the connection between group and subgroup requires a matrix called transformation matrix. Transformation from a high symmetry group to a low symmetry group is always expressed by a transformation matrix. This transformation matrix is accompanied with an index.

The two symmetry groups are not necessarily related to each other only by a group-subgroup relation. For example, two symmetry groups having a common subgroup can share part of their symmetry operations in common; or two groups having a common supergroup can have different part of the symmetries of the supergroup [3].

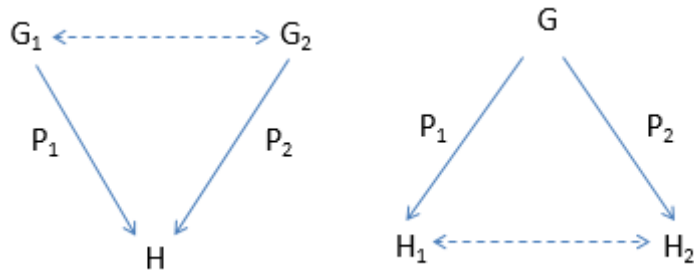


Figure 3.1. Related Groups and Subgroups

3.2. Index

Index is an integer value that infers relation between groups and subgroups. Index is related to either to translation loss or point group symmetry loss or both of them. High symmetry reduction to low symmetry during symmetry break by means of phase transition expresses a mathematical relation. This relation shows allowed transition between the symmetry groups. There are the translationengleiche index and the klassengleiche index (discussed in Section 7.1.1 and Section 7.1.2).

If index, $[i]$, is a prime number, there can be no intermediary group between G and H ;

$$[i] = (\text{order of } G)/(\text{order of } H)$$

$$i = \frac{|G|}{|H|}$$

Figure 3.2 shows an example of subgroups chain. Index between G and H can be calculated by the multiplication of the index between G and Z_1 and the index between Z_1 and H .

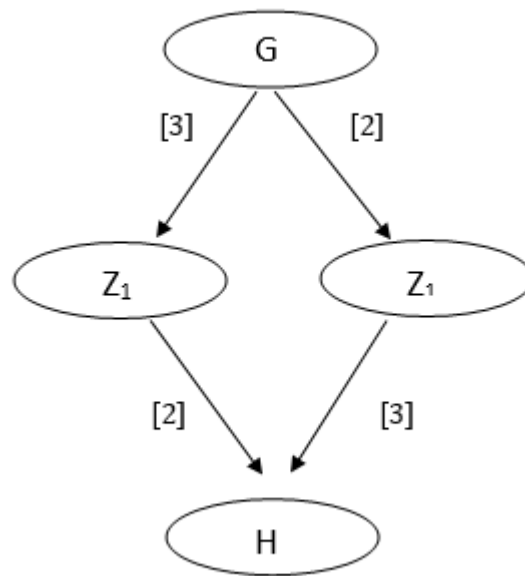


Figure 3.2. Subgroup Chain

Hermann's theorem claims that if a subgroup is a maximal subgroup of the group, it is either a *klassengleiche* subgroup (loss of translation symmetry) or a *translationengleiche* subgroup (loss of point group symmetry).

3.3. Conjugacy Class

Let H and H' be subgroups of the group G and that they satisfy the following condition:

$$H' = g_m^{-1} H g_m, g_m \in G \text{ and } g_m \notin H$$

Then, H and H' are called *conjugate subgroups* in G .

g_m may not be the only element of the group which transforms H to H' ; there may exist several elements of G which can result in the same conjugacy relation. When all elements of the G are run, the set of all elements which are conjugate to H is called the conjugacy class [3].

3.4. Conjugate Subgroups

There can be conjugate subgroups of a space group. Let H and H' be subgroups of G and H' be conjugate to H in G . Conjugacy class formed by H and H' states that [3]:

- H and H' belong to the same space group,
- H and H' have the same lattice dimensions,
- H and H' have equivalent symmetry operations in G .

Maximal subgroups H and H' can be conjugate in G in two ways [3]:

- 1- **Oriental Conjugation:** The conjugate subgroups have different orientation of the unit cells, and their axes can intersect by applying symmetry operations of G . These symmetry operations are the conjugate subgroups lost in transformation. Translationengleiche maximal subgroups can be conjugate in minimal supergroup in only orientational conjugation way.
- 2- **Translational Conjugation:** Enlargement of a primitive unit cell of a minimal supergroup G , by a factor of 3 or higher, may generate conjugate subgroups. Conjugate subgroups lose translational symmetry operators thus ending up having larger unit cell than group G . Taking different parts of repeating elements of G creates conjugate subgroups and they can be distinguished by their position of the origins. Their origins can be mapped onto each other by applying translational symmetry operators of G .
If the origin of the unit cell of G is not fixed by symmetry (floatable) in a direction, then enlargement in that direction does not result in conjugate subgroups. Translational conjugation may occur among klassengleiche and isomorphic maximal subgroups.

3.5. Normalizers

In addition to g_m , the element of the group G , that maps two conjugate subgroups onto each other, there exist further elements g_i , and these elements can map the subgroup H onto itself.

$$H = g_i^{-1} H g_i, g_i \in G$$

The set of g_i includes the elements of the H , but there may exist further elements which provide the relation above. The group consisting of all the elements g_i is called the *normalizer* of H in G .

$$N_G(H) = \{g_i \in G \mid g_i^{-1} H g_i = H\}$$

Normalizer is an intermediate group between the group and the subgroup.

$$H \leq N_G(H) \leq G$$

Euclidean Normalizer: It is a special group that represents a normalizer group between space group G and supergroup \mathcal{E} . The elements of \mathcal{E} can map the G onto itself. All space groups are subgroups of their corresponding \mathcal{E} .

Affine Normalizer: In addition to mapping a space group onto itself, the affine normalizer allows the lattice to expand or compress. Euclidean normalizer is a subgroup of the affine normalizer.

Chirality-preserving Euclidean Normalizer: Chirality-preserving Euclidean normalizer is a subgroup of Euclidean normalizer not including inversion, rotoinversion, reflection and glide reflection operators.

$$G \leq N_{\mathcal{E}^+}(G) \leq N_{\mathcal{E}}(G)$$

If Euclidean normalizer $N_{\mathcal{E}}(G)$ is non-centrosymmetric, then chirality-preserving Euclidean normalizer is identical to Euclidean normalizer [3].

3.6. Coset Decomposition

If $H < G$, then G can be decomposed in terms of H .

Let $G = \{g_1, g_2, g_3, g_4, \dots, g_i\}$ and $H = \{h_1, h_2, h_3, h_4, \dots, h_j\}$

$$g_1 = h_1 = I$$

H, g_2H, g_3H etc. represent left cosets (if $g_3 \notin g_2H$) and similarly H, Hg_2, Hg_3 etc. represent right cosets of group G .

Let g_j represents the elements of G that forms new cosets with respect to H .

Left coset decomposition; $G = IH + \sum_{j=2}^m g_jH$

Right coset decomposition; $G = IH + \sum_{j=2}^m Hg_j$

m shows number of cosets i.e. index $[i]$ of H in G , $m \leq i$

Properties of Coset Decomposition [2]:

1. Each symmetry element of G appears in only one coset.
2. Number of elements in a coset is equal to the order of H .
3. The number of left cosets and right cosets are equal and this number shows the index of H in G , $[i]$.
4. Only one of the cosets represents the subgroup, H .
5. When left and right cosets are same, the subgroup is called *normal subgroup*. Otherwise, subgroup belongs to *conjugate subgroup*.

Lagrange's Theorem states that groups that have prime order have no proper subgroups (i.e. $H \subset G, H \neq G \rightarrow H < G$).

$$|H| = \text{order of } H$$

$$|G| = \text{order of } G$$

$$[i] = |G| / |H|$$

3.7. Transformation Matrix

As previously stated, relations between different structures e.g., group-subgroup relations are identified by a matrix called the transformation matrix.

Transformation can be used in two fundamental ways in crystallography. First aspect is used to define transformations of the coordinate system and the unit cell. When comparison of different settings of monoclinic, orthorhombic and rhombohedral space groups is considered, unit cell transformation is specifically revealed. Expressing the phase transitions and group-subgroup relations by a transformation matrix referred by a transformed coordinate system is useful for non-conventional crystal structures. Secondly, transformation may express a change of coordinate of a point without changing the coordinate system. This is related to symmetry operations of crystal structures [6].

Briefly, changing the coordinate system is necessary for the following cases [3]:

1. For comparison of two same crystal structures that have been described in different coordinate systems (due to such as identification through different experimental processes & instruments), transformation of the coordinate system is required. Also to investigate the group-subgroup relation of two space groups having been described in different coordinate systems, transformation of the coordinate system is necessary.
2. Phase transitions are generally described in conventional data and it is convenient to transform the high symmetry phase structure into the settings of the low symmetry (high symmetry phase's non-conventional settings) phase for their comparison.
3. Orthonormal bases are more desirable to use than conventional bases to describe physical data (such as elasticity, thermal conductivity, etc.) in crystallography. So, point coordinates, indices of planes and directions

have to be converted to orthonormal bases whenever possible to be compared to those data from literature.

Origin shift and change of bases can be represented by a matrix pair (P, p) . P is (3×3) square matrix representing changes in bases and p column matrix describes the origin shift. Their combined matrix pair (P, p) corresponds to the transformation matrix.

Let $(\mathbf{a}, \mathbf{b}, \mathbf{c})$ be the basis vectors of a space group G and O is the origin.

Origin shift can be described by;

$$O' = O + p$$

O' corresponds to the new origin of the new coordinate system.

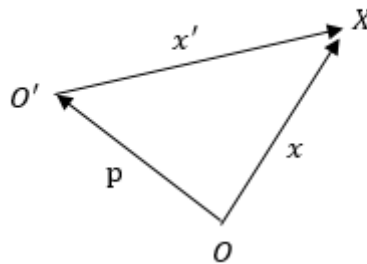


Figure 3.3. Origin Shift

Column vector x consist of coordinates of the point X with respect to O and column vector x' shows coordinates of the point X in new coordinate system O' .

Considering Figure 3.3, we can write:

$$p = \overrightarrow{OO'}$$

$$x' = \overrightarrow{O'X}$$

$$x = \overrightarrow{OX}$$

Then, we can obtain:

$$x' = x - p$$

So, the transformed coordinates of the point can be rewritten as:

$$x' = (I, -p)x = (I, p)^{-1}x$$

Now, we can consider the change of matrix pair (W, w) of group G in the new coordinate system as using the equation we obtained in Section 1.3

$$x'' = (W_2, w_2)x'$$

We obtain:

$$\begin{aligned} (I, -p)x' &= (W_2, w_2)(I, -p)x \\ x' &= (I, -p)^{-1}(W_2, w_2)(I, -p)x \end{aligned}$$

From here, we can derive the following equation by using $x' = (W, w)x$ in the previous equation.

$$(W, w) = (I, -p)^{-1} (W_2, w_2)(I, -p)$$

Since $(I, -p) = (I, p)^{-1}$, we can obtain the (W_2, w_2) matrix pair after the origin shift.

$$(W_2, w_2) = (I, p)^{-1}(W, w)(I, p)$$

Decomposition of the equation shows:

$$W_2 = W \text{ and } w_2 = w + (W - I)p$$

Above expression shows that there is no change in column part W by origin shift. If W equals to unit matrix, $W = I$, then there will be no change in translation part, either.

Transformed basis vectors $(\mathbf{a}' \mathbf{b}' \mathbf{c}')$ is obtained by linear combination of old basis vectors $(\mathbf{a} \mathbf{b} \mathbf{c})$ and (3×3) transformation matrix P .

$$(\mathbf{a}' \mathbf{b}' \mathbf{c}') = (\mathbf{a}, \mathbf{b}, \mathbf{c})P$$

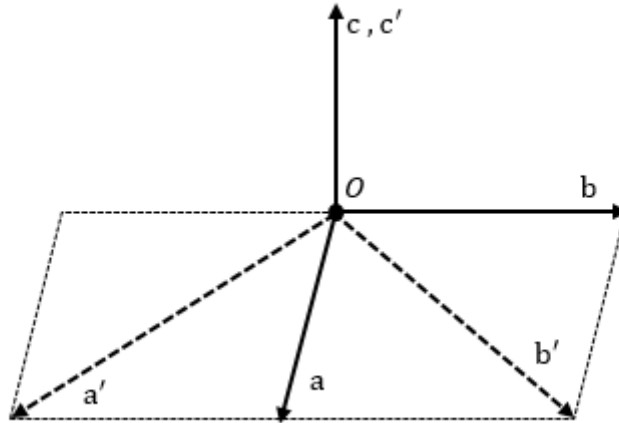


Figure 3.4. Change of Basis

Example: In Figure 3.4, basis vectors $(\mathbf{a} \ \mathbf{b} \ \mathbf{c})$ are transformed to new basis $(\mathbf{a}' \ \mathbf{b}' \ \mathbf{c}')$ by a matrix P . Symmetry operators and point coordinates are transferred to the new basis.

$$\mathbf{a}' = \mathbf{a} - \mathbf{b}$$

$$\mathbf{b}' = \mathbf{a} + \mathbf{b}$$

$$\mathbf{c}' = \mathbf{c}$$

Then, the (3×3) transformation matrix P is written as;

$$P = \begin{pmatrix} 1 & 1 & 0 \\ -1 & 1 & 0 \\ 0 & 0 & 1 \end{pmatrix}$$

3.8. Metric Tensor

Metric parameters consist of lengths of the basis vectors and the intervector angles. Let $(\mathbf{a}, \mathbf{b}, \mathbf{c})$ be basis vectors in 3 dimension. Then, scalar products of all pairs of the basis vectors can be collected in a (3×3) matrix called the *metric tensor* [7].

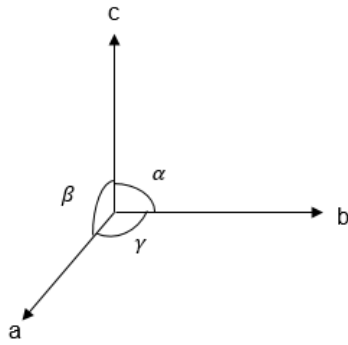


Figure 3.5. Intervector Angles in 3D

Metric tensor can be easily written with lattice parameters of a crystal consisting of the basis lengths and the angles between non-coplanar vectors.

$$G = \begin{pmatrix} \vec{a}\vec{a} & \vec{a}\vec{b} & \vec{a}\vec{c} \\ \vec{b}\vec{a} & \vec{b}\vec{b} & \vec{b}\vec{c} \\ \vec{c}\vec{a} & \vec{c}\vec{b} & \vec{c}\vec{c} \end{pmatrix}$$

Transformation of a basis to another one can be derived by transformation matrix \mathbf{P} . Similar relation holds for the metric tensor and transformed metric tensor.

$$G' = \mathbf{P}^T \mathbf{G} \mathbf{P}$$

II. GROUP THEORY IN SOLID STATE PHYSICS

4. POINT GROUPS

Crystallographic point groups represent finite-dimensional groups containing reflection and rotation symmetry operators that leave a common point fixed under applications of the respective operator. There are 32 crystallographic point groups as classified in Table 4.1. Comprehensive approach to the 'point group' term requires dealing with site symmetry (as mentioned in this study) in crystals and external shape of ideally developed macroscopic crystals in order to avoid confusion [8] [3] [9].

Table 4.1. Three Dimensional Crystal Systems and Point Groups [10]

Crystal System	Point Groups
Triclinic	$1, \bar{1}$
Monoclinic	$2, m, 2/m$
Orthorhombic	$222, mm2, mmm$
Tetragonal	$4, \bar{4}, 4/m, 422, 4mm, \bar{4}2m, 4/mmm$
Trigonal	$3, \bar{3}, 32, 3m, \bar{3}m$
Hexagonal	$6, \bar{6}, 6/m, 622, 6mm, \bar{6}2m, 6/mmm$
Cubic	$23, m\bar{3}, 432, \bar{4}3m, m\bar{3}m$

Consider a system (that does not repeat itself, i.e., without translational symmetry), consisting of a finite number of atoms, which maps onto itself by the set of isometries. The set of all symmetry operations constitutes to the point group of the system. Site symmetry of a point consists of all the point group symmetry operations that leave that point in the system unchanged [11]. The number of operators in a site symmetry set is equal to the ratio of the number of point group operators to the multiplicity of the point.

The point group symbol can be obtained by reducing the glide planes of the space group to mirror planes and screw axes of the space group to rotation axes [12]. Equivalently, one can obtain the point group operators of a space group by discarding all the translational components.



5. BRAVAIS LATTICES

There are 14 possible three dimensional Bravais lattices exhibiting symmetry features. These Bravais lattices are classified in 7 crystal systems by the angles and length of the primitive translations [13]. There are 5 Bravais lattices in two dimensions and 1 in one dimension. Bravais lattice shows the arrangement of the bases in a unit cell [14].

Two lattices belong to the identical Bravais lattice group as long as they coincide within their point group symmetry and centering mode of their units. Therefore, same crystal family may have various Bravais types by centering modes. Otherwise, lattices can be classified according to their domain topology, called Voronoi types. There are 5 types of lattices in three dimensions with respect to Voronoi classification. If topological and symmetry properties appear in classification, 24 *Symmetrische Sorten* types appear in three dimensions [7].

Table 5.1. Crystal Systems and Bravais Lattices

	Crystal System	Bravais Lattices	Conditions
1	Triclinic	Primitive	$a \neq b \neq c$ $\alpha \neq \beta \neq \gamma \neq 90^\circ$
2	Monoclinic	Primitive Base centred (one face centred)	$a \neq b \neq c$ $\alpha = \gamma = 90^\circ \neq \beta \neq 90^\circ$
3	Orthorhombic	Primitive Base centred Face centred Body centred	$a \neq b \neq c$ $\alpha = \beta = \gamma = 90^\circ$
4	Tetragonal	Primitive Body centred	$a = b \neq c$ $\alpha = \beta = \gamma = 90^\circ$
5	Hexagonal	Primitive	$a = b \neq c$ $\alpha = \beta = 90^\circ \neq \gamma = 120^\circ$
6	Trigonal (Rhombohedral)	Primitive	$a = b \neq c$ $\alpha = \beta = 90^\circ \neq \gamma = 120^\circ$
7	Cubic	Primitive Face centred Body centred	$a = b = c$ $\alpha = \beta = \gamma = 90^\circ$

5.1. Triclinic

In this system, crystals consist of unequal three axes inclining with oblique angles with respect to each other. Triclinic crystal structure has the lowest symmetry among all unit cells containing only 1 and $\bar{1}$ point group symmetries which are both cyclic. Unit cell of triclinic system is represented in primitive type and positioned as contacting 8 Bravais lattice points on the corners. 8% percentage of all minerals belongs to this system [15]. Rhodonite ($[\text{Mn, Fe, Mg, Ca}]\text{SiO}_3$) is an example of triclinic crystal system having $\bar{1}$ symmetry axis [15] [10].

5.2. Monoclinic

As in triclinic system, monoclinic system has three unequal edges and two axes being perpendicular to each other while the remaining angle is oblique. Monoclinic crystal system has 2, m and $2/m$ point groups of which the first two are cyclic. Point group 2 represents the 2-fold symmetry along b-axis, while m always refers to a vertical mirror plane containing either the a-axis or the c-axis. 27% of all known minerals crystallize in this system and most of them have $2/m$ point group symmetry [10]. Aegerine mineral ($\text{NaFeSi}_2\text{O}_6$) crystallizes in monoclinic system with $2/m$ site symmetry [15].

5.3. Orthorhombic

Orthorhombic system is described by vectors of three perpendicular axes having unequal length. This crystal system has 4 Bravais lattices; primitive, body-centred, base-centred and face centred. It can be confusing when β axial angle of monoclinic unit cell is very close to 90° , when it may be seen as pseudo-orthorhombic system. Orthorhombic crystal system can be distinguished by the 2-fold symmetry axes that hold its own shape under 180° rotating of cell along c-axis. In this case, primitive and base-centred lattices exchange their centering type. Similarly, body-centred and face-centred unit cells swap their alignment. Orthorhombic system has $mm2$, 222 and mmm point group symmetries. Baryte (BaSO_4) is an example of the crystal having monoclinic structure with $2/m 2/m 2/m (mmm)$ symmetry [15] [10].

5.4. Tetragonal

In this system, crystals are expressed by three perpendicular axes, two of which have equal length. Tetragonal crystal system can be distinguished by the four-fold symmetry axes that overlap the atoms onto themselves by a 90° rotating of cell. Tetragonal system consists of primitive and body-centred Bravais lattices. As an example, Apophyllite ($[\text{K,Na}]\text{Ca}_4\text{Si}_8\text{O}_{20}[\text{F,OH}]$) crystallizes in tetragonal structural system with $4/m\ 2/m\ 2/m\ (4/mmm)$ point group symmetry [15] [10].

5.5. Hexagonal

Hexagonal crystal system has four axes, three of equal horizontal axes at 120° to each other. The other axis is perpendicular to the other three. Rotating the unit cell by 60° holds the atom positions same without changing their appearance. The fewest substances are assigned to hexagonal crystal system. Vanadinite ($\text{Pb}_5(\text{VO}_4)_3\text{Cl}$) ($6/m$) and graphite have structures belonging to the hexagonal system [15] [10].

5.6. Trigonal (Rhombohedral)

Rhombohedral crystal system is also called trigonal system and can be considered as a subdivision of hexagonal system. The unit cell in this system has 3-fold symmetry by means of rotating the cell by 120° results in same appearance of the atoms. Calcite (CaCO_3) ($\bar{3}2/m$) and Selenium crystallizes in this form [15] [10].

5.7. Cubic

The cubic crystal system has the highest symmetry. It also has the greatest number of restrictions. Not only do all the angles equal 90° , but all the sides have the same length as well. There are three Bravais lattices with cubic symmetry; primitive, body-centred and face-centred. Fluorite (CaF_2) crystallizes in cubic form with $4/m\bar{3}2/m$ site symmetry [15] [10].

5.8. Unit Cell, Primitive Cell, Centring Factor

Unit cell is the basic repeating parallelepiped unit (in 3 dimensions) having all symmetries of the crystal structure. Coordinates of all points inside the unit cell must obey the condition, meaning that atomic positions are normalized (also called “direct” or “fractional” coordinates) [3];

$$0 \leq \{x, y, z\} < 1$$

Geometry of particles in the unit cell identifies the structure of a crystal. Sides of a unit cell describe the basis vectors **a**, **b**, **c**. Magnitudes of the basis vectors and the angles between them shown in Figure 3.5 constitute to the lattice parameters of a crystal [10].

Primitive unit cell is an arrangement of a unit cell by located lattice points just on the corners. Primitive unit cell contains only one lattice point. Conventional bases are the bases used in International Tables Volume A to introduce crystallographic bases. There is no need to identify conventional bases in primitive lattice since bases are chosen to ease calculations as they are parallel to symmetry axes.

Table 5.2. Unit Cell Centring

Centring Symbol	Centring Type	Centring Factor	Coordinates of Lattice Points
P	Primitive	1	0,0,0
C	C-face centred	2	$P + \frac{1}{2}, \frac{1}{2}, 0$
A	A-face centred	2	$P + 0, \frac{1}{2}, \frac{1}{2}$
B	B-face centred	2	$P + \frac{1}{2}, 0, \frac{1}{2}$
I	Body-centred	2	$P + \frac{1}{2}, \frac{1}{2}, \frac{1}{2}$
F	Face centred	4	$P + 0, \frac{1}{2}, \frac{1}{2}; P + \frac{1}{2}, 0, \frac{1}{2}; P + \frac{1}{2}, \frac{1}{2}, 0$
R	Rhombohedrally-centred	3	$P + \frac{2}{3}, \frac{1}{3}, \frac{1}{3}; P + \frac{1}{3}, \frac{2}{3}, \frac{2}{3}$

Lattices are called centred when their conventional basis selection is not primitive. In other words, non-primitive unit cell has more than one lattice point in it. Table 5.2 shows centring symbols, centring types, centring factors and corresponding lattice points in unit cells. Centring factor indicates the number of lattice points in a conventional unit cell.

5.9. Pearson Symbol

Pearson symbol is used to define and classify crystal structures according to their features. Pearson symbol consists of three parts constituted from an italicized lower-case letter, an italicized capital letter and a number, respectively. Lower-case letter indicates the crystal system (e.g., *m* for monoclinic), and capital letter indicates the centring of lattices (e.g., *P* for primitive lattice) and the numerical part points to the number of atoms in the conventional unit cell [16].

Table 5.3. Pearson Symbols of Bravais Lattices

	Crystal System	Bravais Lattices	Pearson Notation
1	Triclinic	Primitive	<i>aP</i>
2	Monoclinic	Primitive Base centred (one face centred)	<i>mP</i> <i>mC, mA, mB</i>
3	Orthorhombic	Primitive Base centred Face centred Body centred	<i>oP</i> <i>mC, mA, mB</i> <i>oF</i> <i>oI</i>
4	Tetragonal	Primitive Body centred	<i>tP</i> <i>tI</i>
5	Hexagonal	Primitive	<i>hP</i>
6	Rhombohedral	Primitive	<i>hR</i>
7	Cubic	Primitive Face centred Body centred	<i>cP</i> <i>cI</i> <i>cF</i>

Pearson symbol does not define a unique space group for a crystal i.e., two different crystal structures belonging to different space groups may be designated to the same Pearson symbol. The following example shows this ambiguity due to Pearson notation.

Example: Both Al₃Zr and SeTl structures have tetragonal crystal system with body-centred unit cell.

Crystal Structure	Al ₃ Zr	SeTl
Space Group	I4/mmm	I4/mcm
Space Group Number	139	140
Pearson Symbol	<i>tI16</i>	<i>tI16</i>

6. SPACE GROUPS

Space group is formed by the set of all symmetry operators of an object. In other words, space group shows the symmetry group of a three-dimensional crystal. There are 230 space groups identified by the combination of 32 point group symmetries and 14 Bravais lattices. Each crystal belongs to one of these space groups according to the match of its structural properties with the space group constraints.

Table 6.1. Space Groups with Corresponding Crystal System Numbers

Crystal System	Space Group Examples	# of Space Groups	ITA Space Groups Range
Triclinic	$P1, P-1$	2	1,2
Monoclinic	$P2, P2_1, C2, C2/m$	13	#3 - #15
Orthorhombic	$P222, Amm2, Fmmm$	59	#16 - #74
Tetragonal	$P4, I4, I4_1/a$	68	#75 - #142
Trigonal	$P3, R-3c, P-3m1$	25	#143 - #167
Hexagonal	$P6, P6mm, P6_3/mcc$	27	#168 - #194
Cubic	$P23, Fd-3, I2_13$	36	#195 - #230

6.1. Hermann-Mauguin Notation

Hermann-Mauguin notation is a way to identify the symmetries indicating the coordinate system choice. In this notation, a number of 2,3 or 4 symbols are used to specify the space group symmetries. The first symbol is always an upper-case letter indicating the centring of the Bravais lattice. The remaining symbols show the point group symmetry with additional information of glide planes and screw rotation axis since point group symmetry doesn't include glide plane and screw axis.

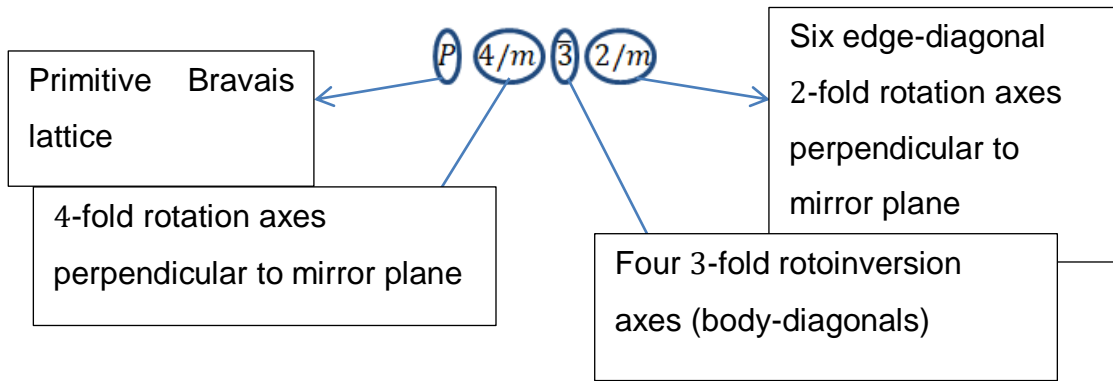
In Hermann-Mauguin notation [15];

1. 1,2,3,4 and 6 express the rotational symmetry axis, e.g. 4 indicates 4-fold rotation and $\bar{1}, \bar{2}, \bar{3}, \bar{4}$ and $\bar{6}$ indicate rotoinversion. For example, $\bar{3}$ refers to a rotation of 120° followed by inversion with respect to the center.
2. The letters m,e,a,b,c,n refers to mirror and glide planes.
3. The / sign has a meaning of “perpendicular to”. For example, $C2/m$ monoclinic system has rotational symmetry axes perpendicular to the mirror plane. However, $R3m$ has 3-fold rotational symmetry axes parallel to the mirror plane.
4. The symbols with a subscripted number e.g. $3_2, 2_1$ indicates screw symmetry. For example, 3_2 symbol implies a rotation of 120° followed by a translation order of $2/3$ along the indicated axis.

Table 6.2. Principal Directions of the Point Groups

Crystal System	Point Groups	Primary Direction	Secondary Direction	Ternary Direction
Triclinic	$1, \bar{1}$	-	-	-
Monoclinic	$2, m, 2/m$	[100]	-	-
Orthorhombic	$222, mm2, mmm$	[100]	[010]	[001]
Tetragonal	$4, \bar{4}, 4/m, 422, 4mm, \bar{4}2m, 4/mmm$	[001]	[010], [100]	[0-10], [110]
Trigonal	$3, \bar{3}, 32, 3m, \bar{3}m$	[001]	[010], [100], [-1-10]	-
Hexagonal	$6, \bar{6}, 6/m, 622, 6mm, \bar{6}2m, 6/mmm$	[001]	[010], [100], [-1-10]	[1-10], [120], [-2-10]
Cubic	$23, m\bar{3}, 432, \bar{4}3m, m\bar{3}m$	[100] [010] [001]	[111], [1-1-1], [-1-1-1], [-1-11]	[1-10], [110], [01-1], [011], [-101], [101]

Example: Hermann-Mauguin notation of the space group (#221) is defined as; $Pm\bar{3}m$. Its extended notation is $P4/m\bar{3}2/m$. Each symbol will be analyzed in order to understand Hermann-Mauguin decoding.



Hermann-Mauguin notation of the point groups' part consists of three principal directions. $4/m$ shows primary direction, $\bar{3}$ shows secondary and $2/m$ shows ternary direction. Related principal directions are shown in Table 6.2.

6.2. Classification of Symmetry Operations

Determinant and trace of the (W, w) pair are the main invariants of isometry. While matrix part of the pair, W , depends on the basis only, column part, w , depends on the selection of both basis and origin [2].

Table 6.3 shows the characterization of W with respect to its trace and determinant. "Type" row represents Hermann-Mauguin point groups' notations. The odd rotoinversion operators $\bar{1}$ and $\bar{3}$ contains inversion operator resulting in the doubling their orders.

Table 6.3 Characterization of the Matrix W [2]

	$\det(W) = +1$					$\det(W) = -1$				
<i>tr</i>(W)	3	2	1	0	-1	-3	-2	-1	0	1
Type	1	6	4	3	2	$\bar{1}$	$\bar{6}$	$\bar{4}$	$\bar{3}$	m
Order	1	6	4	3	2	2	6	4	6	2

6.2.1. Identity

Identity; $I, (I, o)$

$W = I$ (unit matrix), $w = o$ (zero column)

Identity leaves every point of space fixed.

6.2.2. Translation

Translation; $T, (I, t)$

$W = I$; $w = t$ (coefficients of the lattice translation vector)

There is no fixed point, shift of entire point space.

6.2.3. Rotation or Screw Rotation

$\det(W) = +1$; $\text{tr}(W) = 1 + 2\cos\phi < 3$ (ϕ : rotation angle)

Rotation; one line fixed rotation axis.

Screw rotation; no fixed point screw axis. Screw operation is a combination of rotation and translation operators. Symmetry notation is n_p representing the n -fold rotation around the axis by an angle of $360^\circ/n$ and translation along the axis by p/n where p is a positive integer which is less than n [10].

6.2.4. Inversion

Inversion; $(-I, w)$ or $(-1, w)$ or $(\bar{1}, w)$

$W = -I$

Exactly one fixed point. Inversion, $-I$, inverts the space with respect to the center of inversion (fixed point).

6.2.5. Rotoinversion

$\det(W) = -1, W^2 \neq I$

Rotoinversion can be decomposed into a rotation with $-I$.

Exactly one fixed point. Rotoinversion axis intersects the fixed point.

6.2.6. Reflection or Glide Reflection

$\det(W) = -1$, $W^2 = I$ but $W \neq -I$

Reflection; $(W, w)^2 = (I, 0)$; mirror plane of fixed point.

Glide reflection; $(W, w)^2 = (I, t)$, $t \neq 0$

No fixed point. Glide reflection isometry can be decomposed into a reflection by glide plane and a translation by glide vector.

6.3. Site symmetry

Site symmetry corresponds to point group symmetries in a space group. Higher site symmetry has lower multiplicity and space groups are named with the higher site symmetry operator. For example; for the monoclinic space group $C2/m$ (#12), C shows centring of the Bravais lattice and $2/m$ is higher site symmetry operator for the space group.

All site symmetries of a group can be generated by the high site symmetry operators. Generally, higher site symmetry is the origin of the unit cell. During symmetry reduction, site symmetry reduces i.e., Wyckoff position of the atoms does not split and atoms are still symmetrically-equivalent. In other case, site symmetry remains the same i.e., Wyckoff position splits [11].

6.4. Wyckoff Position

Crystallographic orbit refers to a set of symmetrically-equivalent points in a group. If coordinates of the points are fixed according to symmetry operations of the space group, then the orbit is called Wyckoff position. Wyckoff position (WP) represents the equivalent points set or atoms in the unit cell by a notation containing one number and a letter e.g., $2d$, where 2 is the multiplicity which represents number of equivalent points in the corresponding orbit, and letter d is an alphabetical label (a, b, c, d, etc.) incremented from the highest site symmetry point (i.e., lowest multiplicity). Each independent set of atoms in a unit cell boundary is described by a WP notation. Letter selection depends on the choice of origin and coordinate system. Wyckoff set includes equivalent WPs having the same site symmetries.

For example, positions of the space group $C2/m$ representing by $2/m$ site symmetry constitute a Wyckoff set, see in Figure 6.1. Similarly, all equivalent positions around 2-fold rotation axis form another Wyckoff set [11][17].

Two sites corresponding to the same Wyckoff position in a structure does not necessarily mean that they belong to the same crystallographic orbit.

Wyckoff Sets of Space Group $C2/m$ (No. 12) [unique axis b]

NOTE: The program uses the default choice for the group settings.

Letter	Mult	SS	Rep.	Equivalent WP
j	8	1	(x, y, z)	j
i	4	m	(x, 0, z)	i
h	4	2	(0, y, 1/2)	gh
g	4	2	(0, y, 0)	gh
f	4	-1	(1/4, 1/4, 1/2)	ef
e	4	-1	(1/4, 1/4, 0)	ef
d	2	2/m	(0, 1/2, 1/2)	abcd
c	2	2/m	(0, 0, 1/2)	abcd
b	2	2/m	(0, 1/2, 0)	abcd
a	2	2/m	(0, 0, 0)	abcd

Figure 6.1 Wyckoff Sets of Space Group $C2/m$ [5]

6.4.1. General Position vs Special Positions

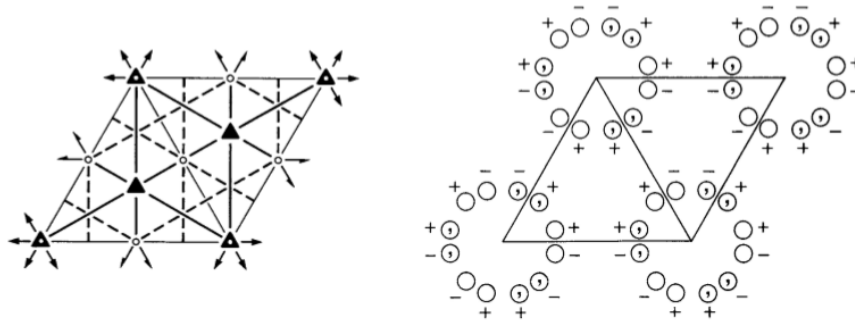
General position represents a set of symmetrically equivalent points in a unit cell on the condition that each point remains invariant only with the application of the identity operator, not by the application of the other symmetry operators. General position refers to the position of the points of a space group with site symmetry 1 such that it has the greatest number of multiplicity [10].

Special position represents a set of symmetrically equivalent points in a unit cell on the condition that each point remains unchanged with the application of the identity operator in addition to at least one more symmetry operator of the

space group. Number of special positions depends on the number and type of site symmetry operators that leave the points unchanged [18] [19].

Multiplicity shows the number of equivalent points in a unit cell of a crystal. Ratio of multiplicity of general position and multiplicity of special position is always an integer. Multiplicity of special position is always less than that of the multiplicity of the general position.

$P\bar{3}m1$ D_{3d}^3 $\bar{3}m1$ Trigonal
 No. 164 $P\bar{3}2/m1$ Patterson symmetry $P\bar{3}m1$



Origin at centre ($\bar{3}m1$)

Asymmetric unit $0 \leq x \leq \frac{2}{3}$; $0 \leq y \leq \frac{1}{3}$; $0 \leq z \leq 1$; $x \leq (1+y)/2$; $y \leq x/2$

Vertices $0,0,0$ $\frac{1}{2},0,0$ $\frac{2}{3},\frac{1}{3},0$
 $0,0,1$ $\frac{1}{2},0,1$ $\frac{2}{3},\frac{1}{3},1$

Symmetry operations

- | | | |
|------------------------|-----------------------------------|-----------------------------------|
| (1) 1 | (2) 3^+ $0,0,z$ | (3) 3^- $0,0,z$ |
| (4) 2 $x,x,0$ | (5) 2 $x,0,0$ | (6) 2 $0,y,0$ |
| (7) $\bar{1}$ $0,0,0$ | (8) $\bar{3}^+$ $0,0,z$; $0,0,0$ | (9) $\bar{3}^-$ $0,0,z$; $0,0,0$ |
| (10) m x,\bar{x},z | (11) m $x,2x,z$ | (12) m $2x,x,z$ |

Figure 6.2. Unit Cell Representation of $P - 3m1$ Space Group and its Symmetry Operations [20]

Generators selected (1); $t(1,0,0)$; $t(0,1,0)$; $t(0,0,1)$; (2); (4); (7)

Positions

Multiplicity,
Wyckoff letter,
Site symmetry

Coordinates

General position

Reflection conditions

General:

no conditions

Special: no extra conditions

12	j	1	(1) x, y, z	(2) $\bar{y}, x - y, z$	(3) $\bar{x} + y, \bar{x}, z$
			(4) y, x, \bar{z}	(5) $x - y, \bar{y}, \bar{z}$	(6) $\bar{x}, \bar{x} + y, \bar{z}$
			(7) $\bar{x}, \bar{y}, \bar{z}$	(8) $y, \bar{x} + y, \bar{z}$	(9) $x - y, x, \bar{z}$
			(10) \bar{y}, \bar{x}, z	(11) $\bar{x} + y, y, z$	(12) $x, x - y, z$

6	i	$.m.$	x, \bar{x}, z	$x, 2x, z$	$2\bar{x}, \bar{x}, z$	\bar{x}, x, \bar{z}	$2x, x, \bar{z}$	$\bar{x}, 2\bar{x}, \bar{z}$
6	h	$.2.$	$x, 0, \frac{1}{2}$	$0, x, \frac{1}{2}$	$\bar{x}, \bar{x}, \frac{1}{2}$	$\bar{x}, 0, \frac{1}{2}$	$0, \bar{x}, \frac{1}{2}$	$x, x, \frac{1}{2}$
6	g	$.2.$	$x, 0, 0$	$0, x, 0$	$\bar{x}, \bar{x}, 0$	$\bar{x}, 0, 0$	$0, \bar{x}, 0$	$x, x, 0$
3	f	$.2/m.$	$\frac{1}{2}, 0, \frac{1}{2}$	$0, \frac{1}{2}, \frac{1}{2}$	$\frac{1}{2}, \frac{1}{2}, \frac{1}{2}$			
3	e	$.2/m.$	$\frac{1}{2}, 0, 0$	$0, \frac{1}{2}, 0$	$\frac{1}{2}, \frac{1}{2}, 0$			
2	d	$3m.$	$\frac{1}{3}, \frac{2}{3}, z$	$\frac{2}{3}, \frac{1}{3}, \bar{z}$				
2	c	$3m.$	$0, 0, z$	$0, 0, \bar{z}$				
1	b	$\bar{3}m.$	$0, 0, \frac{1}{2}$					
1	a	$\bar{3}m.$	$0, 0, 0$					

Special positions

Figure 6.3. General Position and Special Positions of $P - 3m1$ [20]

Figure 6.2 and Figure 6.3 were extracted from the *International Tables for Crystallography, Vol A, (2006)* [20].

Figure 6.3 shows an example of general position and special positions. In this case, general position's multiplicity is 12 showing the maximum number of equivalent points in a crystallographic orbit in the unit cell. As indicated above, multiplicity of special positions (6, 3, 2, and 1) is less than the multiplicity of general position.

Numbers in the parentheses (1), (2) etc. coming before the general position and symmetry operations show a label of relationship between the positions and symmetry operators [10].

6.5. Description of Structures

Description of a structure requires information of the space group number, lattice parameters, number of independent sites in its unit cell, Wyckoff positions of the representative atoms and atomic positions. This information is mandatory to identify and distinguish the structures. In this study, all the analyzed structures are collected by R. Nikolova and V. Kostov-Kytin of the

Institute of Mineralogy and Crystallography, Bulgarian Academy of Sciences [21], and their structural relations are analyzed via Bilbao Crystallographic Server online tools [22] [23] in the format, presented in Figure 6.4.

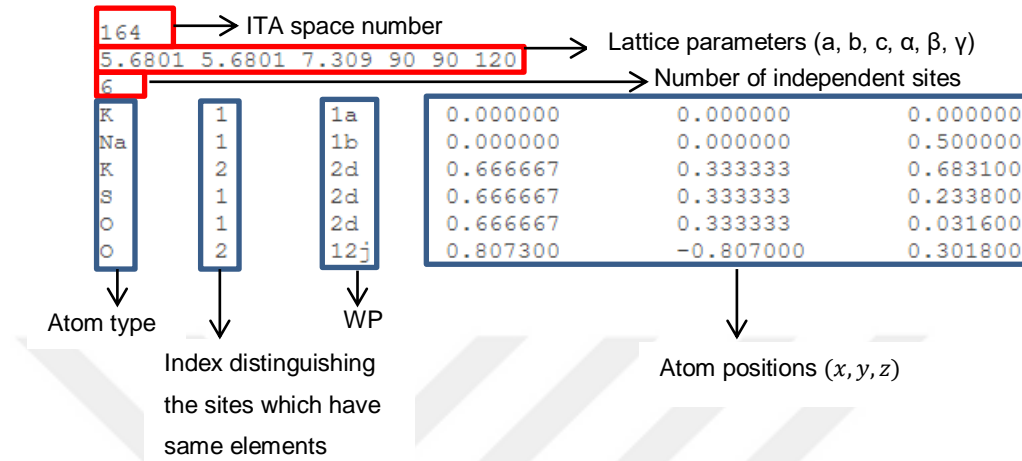


Figure 6.4. Description of a Structure

7. GROUP - SUBGROUP RELATIONS

Correlation of different crystal structures is defined by the relation of the space groups the crystals belong to. This relation implies point groups and lattices of the structures i.e., group-subgroup relations deal with symmetry relations of the space groups.

7.1. Index

Index is a mathematical property that defines the principal relation between groups and subgroups. Index of a subgroup in a supergroup explains roughly how much its unit cell grows or/and the ratio of its point group symmetries loss. Let G be the supergroup and H be its subgroup. Index of H in G is shown as:

$$[G:H] = [i]$$

As mentioned in Section 3.6, the number of left and right cosets is equal, and this number equals to the index of H in G . According to Hermann theorem, if the index is a prime number, it is either a translationengleiche index or a klassengleiche index [11].

A subgroup which is either a translationengleiche subgroup or a klassengleiche subgroup is called a maximal subgroup of its minimal supergroup. From this definition, there cannot be any other intermediate group between the maximal subgroup and the minimal supergroup.

7.1.1. Translationengleiche Index (i_p)

Translationengleiche subgroup (also called t-subgroup) is the maximal subgroup of its minimal supergroup that keeps translational symmetries same while loses some or all point group symmetry operations i.e., they are translational symmetry-equivalent subgroups.

Translationengleiche index is found by the ratio of the number of point group symmetries excluding the translational part.

Translationengleiche index:

$$i_p = \frac{\# \text{ of Symmetry operations of supergroup}}{\# \text{ of Symmetry operations of subgroup}}$$

7.1.2. Klassengleiche Index (i)

Klassengleiche subgroup (also called k-subgroup) keeps point group symmetries unchanged while losing a number of translational symmetries. For example, if a unit cell of a structure grows by 2 times, translational symmetries decreases by 2 times without a loss in point group symmetries (even though the number of translation symmetries of a crystal is infinite, in such a case of doubling its unit cell, it loses odd valued translation operators in a specific direction, hence, halving the number of its translation operators).

Klassengleiche index is found by the ratio of the number of the conventional formula unit per centring factor for the super- and sub-groups (see Section 5.8).

Klassengleiche index formula:

$$i_l = \frac{Z_H}{Z_G} \times \frac{f_C}{f_H}$$

7.2. Transformation Matrix

Transformation matrix expresses the basis changes and origin shift to define the relation between different crystal structures by means of group-subgroup symmetry relations. In other words, transformation matrix represents unit cell transformation upon symmetry reduction. Unit cell transformation is necessary to analyze the group-subgroup relation if group and the subgroup are described in different coordinate systems. Transformation matrix is identified by a matrix pair (P, p) where the (3×3) matrix refers to the change of basis, and the (3×1) column vector represents the origin shift. Transformation matrix is discussed in Section 3.7.

7.3. Wyckoff Position Splitting

Symmetry transformation from a group to its subgroup requires a one-to-one relation of their orbits. Symmetry reduction is not allowed if there is no correlation between Wyckoff positions of the group and the corresponding subgroups. During symmetry reduction, either WP of a supergroup splits into symmetrically-independent positions or its site symmetry operators are reduced, or both cases happen at the same time. Multiplicity of a WP shows the change of the number of the atoms of an orbit in subgroup and the total multiplicity of the group and subgroup gives information of their volume ratio. For example, WP position of a site in a supergroup is 1a and it splits into 2b of a subgroup. Splitting shows that the volume of that subgroup unit cell has grown by 2 times compared to the unit cell of supergroup [3] [11].

7.4. Spontaneous Strain

During the group-subgroup transformation, strain is an essential part in order to describe the plausibility of the phase transition. Comparison of the two structures', that is, the distorted structure's and the reference structure's lattice parameters yields the stress. In other words, incompatibility between the two structures' unit cells gives the degree of lattice distortion. Stress only depends on lattice parameters.

The following relation gives the degree of lattice distortion [24];

$$S = \frac{1}{3} \sqrt{\sum_{i=1}^3 \eta_i^2}$$

where η_i represents the eigenvalues of finite Lagrangian strain tensor $\boldsymbol{\eta}$.

$$\boldsymbol{\eta} = \frac{1}{2}(e + e^T + e^T e) \text{ and } e = R_2 R_1^{-1} - I$$

R_i represents the standard root tensor that transforms conventional coordinate system to the Cartesian bases. In other words, R_i is the root square of the diagonalized metric tensor.

7.5. Bärnighausen Tree

Bärnighausen tree is a useful schematic representation that gives information about a group-subgroup relation. It includes information of Hermann-Mauguin symbols of high symmetry and low symmetry space groups, index and index type of the subgroup, transformation matrix (basis transformation and origin shift) if there is a change, high symmetry and low symmetry crystal structures (name or chemical formula), elements, Wyckoff labels, site symmetries and atomic positions.

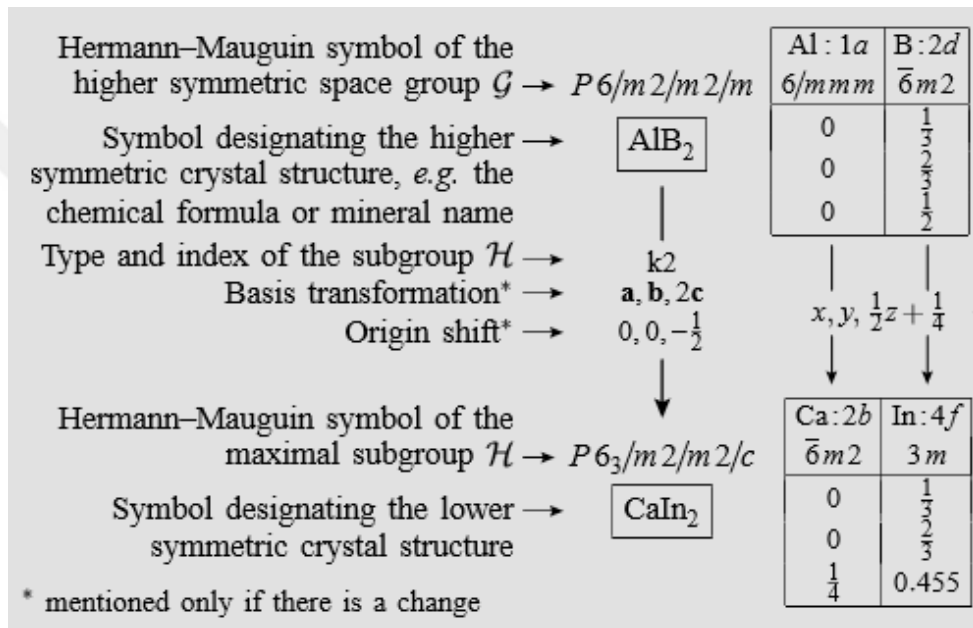


Figure 7.1. Bärnighausen Tree Representing Group-Subgroup Relation [11]

7.6. Case Study

In this section, group-subgroup relation will be analyzed using the phase transformation of $\text{BaNa}(\text{PO}_4)_2$ $P - 3m1 \rightarrow C2/m$ as an example. Transformation matrix, index, atomic orbits, Wyckoff positions splitting and distortion will be calculated. Transition between the crystal $\text{BaNa}(\text{PO}_4)_2$ (Barium Sodium Phosphate) of $P - 3m1$ (#164) space group and the crystal $\text{BaNa}(\text{PO}_4)_2$ of $C2/m$ (#12) space group will be achieved in detail [25].

$$P - 3m1 > C2/m$$

$$G(\#164) > H(\#12)$$

High symmetry structure

164					
5.617	5.617	7.260	90.	90.	120.
6					
Na	1	1a	0.000000	0.000000	0.000000
Ba	1	1b	0.000000	0.000000	0.500000
Ba	2	2d	0.333333	0.666667	0.841800
P	1	2d	0.333333	0.666667	0.282000
O	1	2d	0.333333	0.666667	0.491800
O	2	6i	0.185200	0.814800	0.207000

Figure 7.2. $\text{BaNa}(\text{PO}_4)_2$ ($P-3m1$) (#164) Parameters

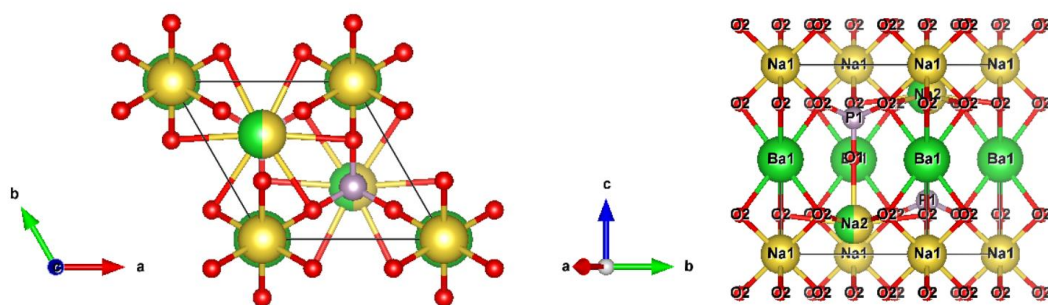


Figure 7.3. $\text{BaNa}(\text{PO}_4)_2$ ($P-3m1$) Structure [26]

Low symmetry structure

```

12
9.743 5.622 7.260 90. 90.10 90.
7
Na 1 2b 0.000000 0.500000 0.000000
Ba 1 2d 0.000000 0.500000 0.500000
Ba 2 4i 0.333200 0.500000 0.158000
P 1 4i 0.165900 0.000000 0.282300
O 1 4i 0.168700 0.000000 0.485500
O 2 4i 0.313600 0.000000 0.210900
O 3 8j 0.093700 0.223300 0.206000

```

Figure 7.4. BaNa(PO₄)₂ (C2/m) (#12) Parameters

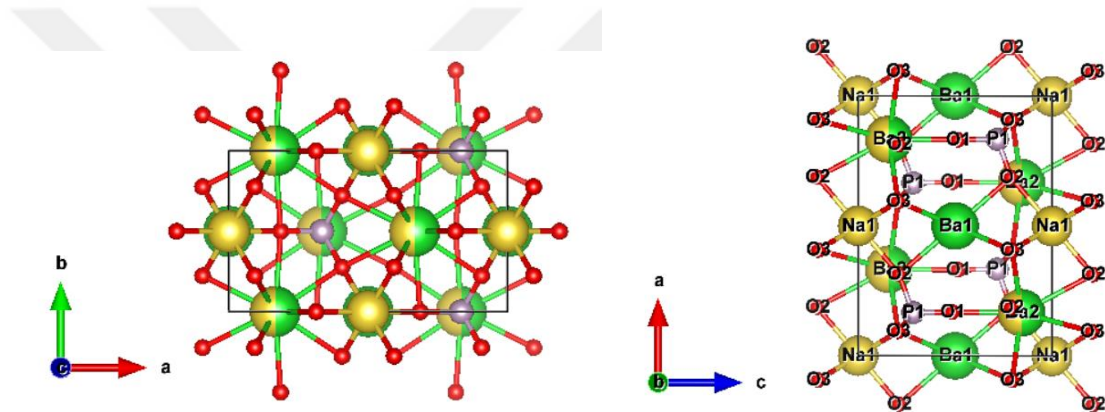


Figure 7.5. BaNa(PO₄)₂ (C2/m) Structure [26]

1. Calculating the Index

To calculate the index in a group-subgroup transformation, it is checked if there is a loss of point group symmetry and/or translation operators. We have to find the klassengleiche index and the translationengleiche index separately.

In order to find the translationengleiche index, we need to know general positions (point group symmetry operations) of the space groups.

Translationengleiche index i_p ;

$$i_p = \frac{\# \text{ of Symmetry operations of } P - 3m1}{\# \text{ of Symmetry operations of } C2/m}$$

The symmetry operations (excluding the translational symmetry operators) of the space group $P - 3m1$ (#164) and $C2/m$ (#12) are given below in Seitz symbol notation, respectively.

$$G(\#164) = \{ \mathbf{1} \mid \mathbf{0} \}, \{ \mathbf{3}^+_{001} \mid \mathbf{0} \}, \{ \mathbf{3}^-_{001} \mid \mathbf{0} \}, \{ \mathbf{2}_{110} \mid \mathbf{0} \}, \{ \mathbf{2}_{100} \mid \mathbf{0} \}, \{ \mathbf{2}_{010} \mid \mathbf{0} \}, \\ \{ -\mathbf{1} \mid \mathbf{0} \}, \{ -\mathbf{3}^+_{001} \mid \mathbf{0} \}, \{ -\mathbf{3}^-_{001} \mid \mathbf{0} \}, \{ \mathbf{m}_{110} \mid \mathbf{0} \}, \{ \mathbf{m}_{100} \mid \mathbf{0} \}, \{ \mathbf{m}_{010} \mid \mathbf{0} \} \quad [5]$$

$$H(\#12) = \{ \mathbf{1} \mid \mathbf{0} \}, \{ \mathbf{2}_{010} \mid \mathbf{0} \}, \{ -\mathbf{1} \mid \mathbf{0} \}, \{ \mathbf{m}_{010} \mid \mathbf{0} \} \quad [5]$$

There are 12 symmetry operations of $P - 3m1$ space group. Excluding the translational part, there are 4 symmetry operations of $C2/m$.

$$i_p = \frac{12}{4} = 3$$

Klassengleiche index can be obtained by estimating the number of the conventional unit per centring factor.

Klassengleiche index i_l ;

$$i_l = \frac{\frac{Z_{C2/m}}{f_{C2/m}}}{\frac{Z_{P-3m}}{f_{P-3m}}} = \frac{\frac{2}{1}}{\frac{1}{1}} = 2$$

$Z_{C2/m}$ and Z_{P-3m} show the number of conventional formula units. Wyckoff positions of the corresponding atoms in high symmetry and low symmetry structures show the ratio of conventional formula unit. For example, high symmetry structure $P - 3m1$ of $\text{BaNa}(\text{PO}_4)_2$ has 1 Na atom while low symmetry structure $C2/m$ of $\text{BaNa}(\text{PO}_4)_2$ has 2. Therefore, the ratio of the conventional unit cells $\frac{Z_{C2/m}}{Z_{P-3m}}$ is found to be 2.

Centring factor f of primitive unit cell; $f_{P-3m} = 1$

Centring factor f of face-centred unit cell $f_{C2/m} = 2$

$$Z_{C2/m} = 4 \text{ and } Z_{P-3m} = 2$$

Thus, from the i_l equation, the klassengleiche index will be:

$$i_l = 1$$

Total index is evaluated by multiplying the translationengleiche index with the klassengleiche index.

$$i = i_p \times i_l = 3$$

It is clearly seen that there are no translations loss in the subgroup, there is only point group symmetry lost in transition. So, $C2/m$ is a translationengleiche subgroup of $P-3m1$. For example, subgroup $C2/m$ does not contain $(-y, -x, z)$ mirror symmetry operation represented as $\{m_{110} | 0\}$ in Seitz notation, while it is contained in the space group $P-3m$.

Since 3 is a prime number, there is no other group between $P-3m1$ and $C2/m$. So, $P-3m1$ (#164) is minimal supergroup of $C2/m$ (#12), and $C2/m$ is maximal subgroup of $P-3m1$.

2. Finding the Transformation Matrix

There might be more than one matrix which refers to the same transformation in different paths when expressing the relations between groups and subgroups. In our case, 3 possible transformation matrices are obtained by using SUBGROUPGRAPH program of Bilbao Crystallographic Server [27]. With index 3, there are 3 transformation matrices corresponding to 3 maximal subgroups of G ($P-3m1$).

$$P_1 = -a + b, -a - b, c; 0,0,0$$

$$P_2 = -a - 2b, a, c; 0,0,0$$

$$P_3 = 2a + b, b, c; 0,0,0$$

In matrix form;

$$P_1 = \begin{pmatrix} -1 & -1 & 0 & 0 \\ 1 & -1 & 0 & 0 \\ 0 & 0 & 1 & 0 \end{pmatrix}$$

$$P_2 = \begin{pmatrix} -1 & 1 & 0 & 0 \\ -2 & 0 & 0 & 0 \\ 0 & 0 & 1 & 0 \end{pmatrix}$$

$$P_3 = \begin{pmatrix} 2 & 0 & 0 & 0 \\ 1 & 1 & 0 & 0 \\ 0 & 0 & 1 & 0 \end{pmatrix}$$

Conjugacy relation states that;

$$H' = g_m^{-1} H g_m, g_m \in G \text{ and } g_m \notin H$$

Then, H and H' are conjugate subgroups and they are symmetrically equivalent.

Figure 7.6 shows a path between H and H' conjugate subgroups.

$$H \rightarrow H': P_2 g_i P_1^{-1}, g_i \in G$$

From conjugacy relation we can write;

$$\begin{aligned} H' &= \underbrace{(P_2 g_i P_1^{-1})^{-1}}_{g_m} H \underbrace{(P_2 g_i P_1^{-1})}_{g_m} \\ &\quad \downarrow \\ H' &= g_m^{-1} H g_m \end{aligned}$$

$P_2 g_i P_1^{-1} \in N_A(G)$, $N_A(G)$ is affine normalizer of group G .

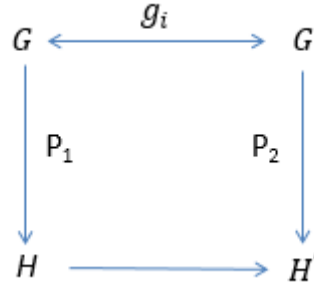


Figure 7.6. Conjugated maximal subgroups of the minimal supergroup

Let H_1, H_2, H_3 be the maximal subgroups of G associated with P_1, P_2, P_3 .

By application of the conjugacy rules to our case, we can check if g_m is an element of G and satisfies the following conditions;

$$\begin{aligned}
 g_m^{-1}H_1g_m = H_2 &\rightarrow (P_2g_iP_1^{-1})^{-1}H_1(P_2g_iP_1^{-1}) = H_2 \\
 g_m^{-1}H_2g_m = H_3 &\rightarrow (P_3g_iP_2^{-1})^{-1}H_2(P_3g_iP_2^{-1}) = H_3 \\
 g_m^{-1}H_1g_m = H_3 &\rightarrow (P_3g_iP_1^{-1})^{-1}H_1(P_3g_iP_1^{-1}) = H_3
 \end{aligned}$$

$(P_2g_iP_1^{-1}), (P_3g_iP_2^{-1})$ and $(P_3g_iP_1^{-1})$ must be the elements of $G (P - 3m1)$ which are lost by the subgroups during the symmetry reduction.

We can apply any of the symmetry operators of the group $G (P - 3m1)$.

For $g_i = x, y, z$

In matrix form:

$$\mathbf{1} = \begin{pmatrix} 1 & 0 & 0 & 0 \\ 0 & 1 & 0 & 0 \\ 0 & 0 & 1 & 0 \end{pmatrix}$$

The element (x, y, z) correspond the identity operation. Calculations are obtained by using GNU Octave [28].

```
>> P2*op1*inv(P1)
ans =
```

$$\begin{pmatrix} 0 & -1 & 0 & 0 \\ 1 & -1 & 0 & 0 \\ 0 & 0 & 1 & 0 \\ 0 & 0 & 0 & 1 \end{pmatrix} \rightarrow (-y, x - y, z) \quad 3^+ 0 0 z \checkmark$$

```
>> P3*op1*inv(P2)
ans =
```

$$\begin{pmatrix} 0 & -1 & 0 & 0 \\ 1 & -1 & 0 & 0 \\ 0 & 0 & 1 & 0 \\ 0 & 0 & 0 & 1 \end{pmatrix} \rightarrow (-y, x - y, z) \quad 3^+ 0 0 z \checkmark$$

```
>> P3*op1*inv(P1)
ans =
```

$$\begin{pmatrix} -1 & 1 & 0 & 0 \\ -1 & 0 & 0 & 0 \\ 0 & 0 & 1 & 0 \\ 0 & 0 & 0 & 1 \end{pmatrix} \rightarrow (-x + y, -x, z) \quad 3^- 0 0 z \checkmark$$

$3^+ 0 0 z$ and $3^- 0 0 z$ satisfy the condition that $g_m \in G$ and $g_m \notin H$.

Thus, the conjugacy relation calculations show that the subgroups H_1, H_2, H_3 are conjugate subgroups of G . They have orientational conjugation since they are translationengleiche subgroups in G as discussed in Section 3.4. Since H_1, H_2, H_3 maximal subgroups are conjugate, any one of the corresponding transformation matrices can be chosen for the rest of the calculations.

Now, it can be proceeded with $P_1 = -a + b, -a - b, c; 0, 0, 0$. P_1 refers to group-subgroup transformation matrix. In order to calculate the overall transformation matrix, affine normalizer and Euclidean normalizer must be found first.

Wyckoff Splitting Compatibility:

By using the selected group-subgroup transformation matrix, correspondence of the Wyckoff positions of the subgroup $H (C2/m)$ corresponding to the Wyckoff positions of $G (P - 3m1)$ can be found. Coordinates of the all Wyckoff positions are available at Bilbao Crystallographic Server [5].

Table 7.1. Wyckoff Positions of P-3m1 [5]

Multiplicity	Wyckoff letter	Site Symmetry	Coordinates
12	j	1	(x, y, z) (-y, x-y, z) (-x+y, -x, z) (y,x,-z) (x-y, -y, -z) (-x,-x+y, -z) (-x, -y, -z) (y,-x+y,-z) (x-y,x,-z) (-y, -x, z) (-x+y,y,z) (x,x-y,z)
6	i	.m.	(x,-x,z) (x,2x,z) (-2x,-x,z) (-x,x,-z) (2x,x,-z) (-x,-2x,-z)
6	h	.2.	(x,0,1/2) (0,x,1/2) (-x,-x,1/2) (-x,0,1/2) (0,-x,1/2) (x,x,0)
6	g	.2.	(x,0,0) (0,x,0) (-x,-x,0) (-x,0,0) (0,-x,0) (x,x,0)
3	f	.2/m	(1/2,0,1/2) (0,1/2,1/2) (1/2 1/2,1/2)
3	e	.2/m.	(1/2,0,0) (0,1/2,0) (1/2,1/2,0)
2	d	3m.	(1/3,2/3,z) (2/3,1/3,-z)
2	c	3m.	(0,0,z) (0,0,-z)
1	b	-3m.	(0,0,1/2)
1	a	-3m.	(0,0,0)

Table 7.1 and Table 7.2 show multiplicity, site symmetries and Wyckoff positions of the space groups ($P - 3m1$) and ($C2/m$), respectively. These are given in conventional settings. Applying group-subgroup transformation matrix to the positions of ($P - 3m1$), it is expected to obtain positions of the ($C2/m$) group.

Table 7.2. Wyckoff Positions of C2/m [5]

Multiplicity	Wyckoff letter	Site Symmetry	Coordinates
8	j	1	(x, y, z) (-x,y,-z) (-x,-y,-z) (x,- y,z)
4	i	m	(x,0,z) (-x,0,-z)
4	h	2	(0,y,1/2) (0,-y,1/2)
4	g	2	(0,y,0) (0,-y,0)
4	f	-1	(1/4,1/4,1/2) (3/4,1/4,1/2)
4	e	-1	(1/4,1/4,0) (3/4,1/4,0)
2	d	2/m	(0,1/2,1/2)
2	c	2/m	(0,0,1/2)
2	b	2/m	(0,1/2,0)
2	a	2/m	(0,0,0)

Group-subgroup transformation matrix is $P_1 = -a + b, -a - b, c; 0,0,0$.

Unit cell of the $\text{BaNa}(\text{PO}_4)_2$ crystal in $(P - 3m1)$ space group has the atomic sites at 1a, 1b, 2d and 6i represented by multiplicity and Wyckoff letters. Low symmetry structure of this case has 2b, 2d, 4i and 8j occupancy. According to Wyckoff splitting rules, 1a of $(P - 3m1)$ must go to 2a of the $(C2/m)$. Similarly, 1b of $(P - 3m1)$ must go to 2c of the $(C2/m)$. However, subgroup has 2b instead of 2a and 2d instead of 2c. This incompatibility can be fixed using Euclidean normalizer to generate alternative but equivalent set of positions.

Euclidean normalizer takes the Wyckoff positions to transformed positions. WYCKSET program of Bilbao Crystallographic Server helps to find the corresponding element of the Euclidean normalizer [5]. Coset representatives of the Euclidean normalizer which transform Wyckoff positions of $C2/m$ are shown in Figure 7.7.

No. #	Coset Representative	Geometrical Interpretation	Transformed WP
1	x,y,z	$\begin{pmatrix} 1 & 0 & 0 & 0 \\ 0 & 1 & 0 & 0 \\ 0 & 0 & 1 & 0 \end{pmatrix}$	1 a b c d e f g h i j
2	$x+1/2,y,z$	$\begin{pmatrix} 1 & 0 & 0 & 1/2 \\ 0 & 1 & 0 & 0 \\ 0 & 0 & 1 & 0 \end{pmatrix}$	$t(1/2,0,0)$ b a d c e f g h i j
3	$x,y,z+1/2$	$\begin{pmatrix} 1 & 0 & 0 & 0 \\ 0 & 1 & 0 & 0 \\ 0 & 0 & 1 & 1/2 \end{pmatrix}$	$t(0,0,1/2)$ c d a b f e h g i j
4	$x+1/2,y,z+1/2$	$\begin{pmatrix} 1 & 0 & 0 & 1/2 \\ 0 & 1 & 0 & 0 \\ 0 & 0 & 1 & 1/2 \end{pmatrix}$	$t(1/2,0,1/2)$ d c b a f e h g i j

Figure 7.7. Transformation of the Wyckoff Positions of $(C2/m)$ via Elements of Euclidean Normalizer

In this case, the Euclidean normalizer element which transforms Wyckoff positions that correspond to low symmetry structure's positions is:

$$N_E = x + \frac{1}{2}, y, z$$

In matrix form;

$$\begin{pmatrix} 1 & 0 & 0 & 1/2 \\ 0 & 1 & 0 & 0 \\ 0 & 0 & 1 & 0 \end{pmatrix}$$

Transformed Wyckoff positions represented by $x + \frac{1}{2}, y, z$ satisfy actual positions of the glaserite-type compound $\text{BaNa}(\text{PO}_4)_2$.

Table 7.3 shows Wyckoff positions of the atoms of the crystal and transformed Wyckoff positions with the application of Euclidean normalizer.

Coordinate system of maximal subgroup is related to minimal supergroup with transformation matrix $P_1 = -a + b, -a - b, c; 0, 0, 0$ and index 3.

Table 7.3. Wyckoff Splitting Compatibility

P3-m1		Group-subgroup Trans. matrix	C2/m			
Atom name	Wyckoff position		Atom name	Wyckoff position	Euclidean normalizer	Transformed wyckoff position
Na	1a	-a+b,-a-b,c;0,0,0	Na	2a	x+1/2,y,z	2b
Ba	1b	-a+b,-a-b,c;0,0,0	Ba	2c	x+1/2,y,z	2d
Ba	2d	-a+b,-a-b,c;0,0,0	Ba	4i	x+1/2,y,z	4i
P	2d	-a+b,-a-b,c;0,0,0	P	4i	x+1/2,y,z	4i
O	2d	-a+b,-a-b,c;0,0,0	O	4i	x+1/2,y,z	4i
O	6i	-a+b,-a-b,c;0,0,0	O	4i+8j	x+1/2,y,z	4i+8j

Lattice Compatibility:

In this case, transformation of a group to a subgroup with possible paths is being studied. This experimentally-observed glaserite-type structure (GTS) does not fit completely with the reference structure (being the high symmetry structure represented in the low symmetry structure's setting via the transformation matrix). Comparison of reference and observed structures reveals another transformation related to lattice expansion and compression that is the affine normalizer. Lattice compatibility transformation matrix is calculated with affine normalizer.

TRANSTRU and COMPSTRU programs of Bilbao Crystallographic Server are used to compare the reference and observed structures of the group $C2/m$ (#12) [29].

Reference Structure (#12)

```
012
9.728930 5.617000 7.260000 90.000000 90.000000 90.000000
8
Na 1 2a 0.000000 0.000000 0.000000
Ba 1 2c 0.000000 0.000000 0.500000
Na 2 4i 0.166667 0.500000 0.841800
Ba 2 4i 0.166667 0.500000 0.841800
P 1 4i 0.166667 0.500000 0.282000
O 1 4i 0.166667 0.500000 0.491800
O 2 4i 0.314800 0.500000 0.207000
O 3 8j 0.592600 0.222200 0.207000
```

Glaserite Structure (#12)

```
12
9.743 5.622 7.260 90. 90.10 90.
8
Na 1 2b 0.000000 0.500000 0.000000
Ba 1 2d 0.000000 0.500000 0.500000
Ba 2 4i 0.333200 0.500000 0.158000
Na 2 4i 0.333200 0.500000 0.158000
P 1 4i 0.165900 0.000000 0.282300
O 1 4i 0.168700 0.000000 0.485500
O 2 4i 0.313600 0.000000 0.210900
O 3 8j 0.093700 0.223300 0.206000
```

Figure 7.8. Reference Structure vs. Glaserite-type Structure of $C2/m$ Space Group

Figure 7.8 shows the difference of lattice parameters and atomic positions between the reference and glaserite-type crystal structures.

There are two transformation options obtained from COMPSTRU program that have the best matches of lattice parameters. These transformations represent the element of the affine normalizer.

$$N_A(1) = a, b, c$$

$$N_A(2) = -a, -b, c$$

Both of them have no effect to change coordinate of the lattices and obey the general formula of affine normalizer of $C2/m$ shown in Figure 7.9.

Overall transformation matrix is found by multiplication of group-subgroup transformation matrix, Euclidean normalizer element and affine normalizer element. Since there are two options for affine normalizer selection, both of them may be applied separately, and then equivalency of the overall matrices may be checked.

(N_1, n_1)	$\begin{bmatrix} u_{11} & 0 & n_{13} \\ 0 & \pm 1 & 0 \\ g_{31} & 0 & u_{33} \end{bmatrix} \begin{bmatrix} 1/2n_1 \\ 1/2n_2 \\ 1/2n_3 \end{bmatrix}$
--------------	--

Figure 7.9. General Formula of Affine Normalizer of $C2/m$ Space Group (unique axis b) (u:odd; n:integer; g:even)

$$P_{overall}(1) = P_1 \times N_A(1) \times N_E$$

$P_1, N_A(1)$ and N_E are in (4×4) augmented matrix form.

$$P_{overall}(1) = \begin{pmatrix} -1 & -1 & 0 & -1/2 \\ 1 & -1 & 0 & 1/2 \\ 0 & 0 & 1 & 0 \end{pmatrix}$$

$$P_{overall}(1) = -a + b, -a - b, c; -\frac{1}{2}, \frac{1}{2}, 0$$

$$P_{overall}(2) = \mathbf{P}_1 \times \mathbf{N}_A(2) \times \mathbf{N}_E$$

$$P_{overall}(2) = \begin{pmatrix} 1 & 1 & 0 & 1/2 \\ -1 & 1 & 0 & -1/2 \\ 0 & 0 & 1 & 0 \end{pmatrix}$$

$$P_{overall}(2) = a - b, a + b, c; \frac{1}{2}, -\frac{1}{2}, 0$$

Transformation matrix, index, distortion and atomic displacement results can be calculated together by using STRUCTURE RELATIONS program of Bilbao Crystallographic Server. The most suitable transformation matrix that connects the structures of group $\text{BaNa}(\text{PO}_4)_2$ and subgroup $\text{BaNa}(\text{PO}_4)_2$ is;

$$P_{SR} = a - b, -a - b, -c; \frac{1}{2}, -\frac{1}{2}, 0$$

$$P_{SR} = \begin{pmatrix} 1 & -1 & 0 & 1/2 \\ -1 & -1 & 0 & -1/2 \\ 0 & 0 & -1 & 0 \end{pmatrix}$$

We have 3 transformation matrices referring a relation between the group and the subgroup. Any one of them is suitable to define transformation between $(P - 3m1)$ and $(C2/m)$ in this case, but equivalency of these matrices will be checked first.

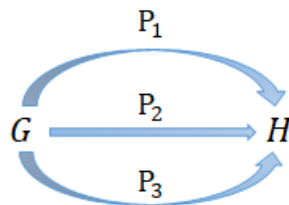


Figure 7.10. Identical Transformation Matrices between the Group and the Subgroups

Figure 7.10 shows transformation paths of the group G to subgroup H with three transformation matrices. P_1, P_2 and P_3 substitute $P_{overall}(1), P_{overall}(2)$ and P_{SR} for this case, respectively. In order to check whether all overall transformation matrices are equivalent or not by the following equality must be provided.

$$P_1 P_2^{-1} = P_2 P_1^{-1}$$

$$P_1 P_3^{-1} = P_3 P_1^{-1}$$

$$P_2 P_3^{-1} = P_3 P_2^{-1}$$

```
>> P1*inv(P2)
ans =
-1  0  0  0
  0 -1  0  0
  0  0  1  0
  0  0  0  1
```

```
>> P2*inv(P1)
ans =
-1  0  0  0
  0 -1  0  0
  0  0  1  0
  0  0  0  1
```

P_1 and P_2 are equivalent

```
>> P1*inv(P3)
ans =
  0  1  0  0
  1  0  0  0
  0  0 -1  0
  0  0  0  1
```

```
>> P3*inv(P1)
ans =
  0  1  0  0
  1  0  0  0
  0  0 -1  0
  0  0  0  1
```

P_1 and P_3 are equivalent

```

>> P2*inv(P3)
ans =
    0  -1  0  0
   -1  0  0  0
    0  0  -1  0
    0  0  0  1

>> P3*inv(P2)
ans =
    0  -1  0  0
   -1  0  0  0
    0  0  -1  0
    0  0  0  1

```

P_2 and P_3 are equivalent

Calculations show that obtained overall matrices are equivalent.

3. Finding Atomic Orbits

It can be proceeded with any one of the overall transformation matrices since they are equivalent. $P_{overall}(1) = P$ will be used for the following calculations.

$$P = \begin{pmatrix} -1 & -1 & 0 & -1/2 \\ 1 & -1 & 0 & 1/2 \\ 0 & 0 & 1 & 0 \end{pmatrix}$$

Atomic positions of the reference structure in the subgroup ($C2/m$) setting are found by the following relation:

$$x' = P^{-1}x$$

x represents atomic position in the unit cell of ($P - 3m1$) and x' represents atomic position of ($C2/m$) subgroup.

Table 7.4. Atomic Positions and Wyckoff Positions of BaNa(PO₄)₂ (#164)

Structure Parameters of BaNa(PO ₄) ₂ (#164)					
Atom type	x	y	z	Occupancy	Wyckoff Position
Na1	0.00000	0.00000	0.00000	1.000	1a
Ba1	0.00000	0.00000	0.50000	1.000	1b
Na2	0.33333	0.66667	0.84180	0.500	2d
Ba2	0.33333	0.66667	0.84180	0.500	2d
P1	0.33333	0.66667	0.28200	1.000	2d
O1	0.33333	0.66667	0.49180	1.000	2d
O2	0.18520	0.81480	0.20700	1.000	6i

For Na1 atom;

$$P^{-1} * Na1(P - 3m1) = Na1'(C2/m)$$

$$P^{-1} = \begin{pmatrix} -1/2 & 1/2 & 0 & -1/2 \\ -1/2 & -1/2 & 0 & 0 \\ 0 & 0 & 1 & 0 \end{pmatrix}$$

$$Na1 = \begin{pmatrix} 0 \\ 0 \\ 0 \end{pmatrix}$$

$$P^{-1} * Na1 = Na1' = \begin{pmatrix} -1/2 \\ 0 \\ 0 \end{pmatrix}$$

(-1/2,0,0) position is representative position of Na1 atom in the subgroup unit cell. In order to find all possible orbits for Na1', all symmetry operators of the subgroup must be applied.


No.	(x,y,z) form	Matrix form	Symmetry operation	
			ITA	Seitz 
(0,0,0) + set				
1	x,y,z	$\begin{pmatrix} 1 & 0 & 0 & 0 \\ 0 & 1 & 0 & 0 \\ 0 & 0 & 1 & 0 \end{pmatrix}$	1	{ 1 0 }
2	-x,y,-z	$\begin{pmatrix} -1 & 0 & 0 & 0 \\ 0 & 1 & 0 & 0 \\ 0 & 0 & -1 & 0 \end{pmatrix}$	2 0,y,0	{ 2 ₀₁₀ 0 }
3	-x,-y,-z	$\begin{pmatrix} -1 & 0 & 0 & 0 \\ 0 & -1 & 0 & 0 \\ 0 & 0 & -1 & 0 \end{pmatrix}$	-1 0,0,0	{ -1 0 }
4	x,-y,z	$\begin{pmatrix} 1 & 0 & 0 & 0 \\ 0 & -1 & 0 & 0 \\ 0 & 0 & 1 & 0 \end{pmatrix}$	m x,0,z	{ m ₀₁₀ 0 }
(1/2,1/2,0) + set click here the show and hide more information				
5	x+1/2,y+1/2,z	$\begin{pmatrix} 1 & 0 & 0 & 1/2 \\ 0 & 1 & 0 & 1/2 \\ 0 & 0 & 1 & 0 \end{pmatrix}$	t (1/2,1/2,0)	{ 1 1/2 1/2 0 }
6	-x+1/2,y+1/2,-z	$\begin{pmatrix} -1 & 0 & 0 & 1/2 \\ 0 & 1 & 0 & 1/2 \\ 0 & 0 & -1 & 0 \end{pmatrix}$	2 (0,1/2,0) 1/4,y,0	{ 2 ₀₁₀ 1/2 1/2 0 }
7	-x+1/2,-y+1/2,-z	$\begin{pmatrix} -1 & 0 & 0 & 1/2 \\ 0 & -1 & 0 & 1/2 \\ 0 & 0 & -1 & 0 \end{pmatrix}$	-1 1/4,1/4,0	{ -1 1/2 1/2 0 }
8	x+1/2,-y+1/2,z	$\begin{pmatrix} 1 & 0 & 0 & 1/2 \\ 0 & -1 & 0 & 1/2 \\ 0 & 0 & 1 & 0 \end{pmatrix}$	a x,1/4,z	{ m ₀₁₀ 1/2 1/2 0 }

Figure 7.11. Symmetry Operators of $C2/m$ [5]

Figure 7.11 shows symmetry operators of the subgroup $C2/m$. With translational part, there are 8 symmetry operators. Na1 atom is positioned in 1a WP for the group $P - 3m1$. In addition to position of Na1' in subgroup unit cell, Wyckoff position splitting will be found by applying all symmetry operators of the subgroup (which can as well be derived from supergroup symmetry operators by applying $W_{sub} = P^{-1}W_{sup}P$) to the representative position of Na1' .

#164 → #12

All possible orbits for Na1';

<u>x</u>	<u>y</u>	<u>z</u>	
-1/2	0	0	$\left. \begin{array}{l} \text{1. } 1/2 \quad 0 \quad 0 \\ \text{2. } 0 \quad 1/2 \quad 0 \rightarrow \text{(#12)} \end{array} \right\} 1a \rightarrow 2b \checkmark$
1/2	0	0	
1/2	0	0	
-1/2	0	0	
0	1/2	0	
1	1/2	0	
1	1/2	0	
0	1/2	0	
0	1/2	0	

Table 7.5. Atomic Positions and Wyckoff Positions of BaNa(PO₄)₂ (#12)

Structure Parameters of BaNa(PO ₄) ₂ (#12)					
Atom type	x	y	z	Occupancy	Wyckoff Position
Na1	0.00000	0.50000	0.00000	1.000	2b
Ba1	0.00000	0.50000	0.50000	1.000	2d
Ba2	0.33320	0.50000	0.15800	0.500	4i
Na2	0.33320	0.50000	0.15800	0.500	4i
P1	0.16590	0.00000	0.28230	1.000	4i
O1	0.16870	0.00000	0.48550	1.000	4i
O2	0.31360	0.00000	0.21090	1.000	4i
O3	0.09370	0.22330	0.20600	1.000	8j

Wyckoff splitting shows that Na1 atom of the group is identified with two separate position coordinate in the subgroup unit cell because of symmetry lost i.e. 1a WP splits into 2b WP. (See Table 7.4 and Table 7.5).


For Ba1 atom;

$$P^{-1} * Ba1(P - 3m1) = Ba1'(C2/m)$$

$$Ba1 = \begin{pmatrix} 0 \\ 0 \\ 1/2 \end{pmatrix}$$

$$P^{-1} * Ba1 = Ba1' = \begin{pmatrix} -1/2 \\ 0 \\ 1/2 \end{pmatrix}$$

All possible orbits for Ba1';

<u>x</u>	<u>y</u>	<u>z</u>	
-1/2	0	1/2	
1/2	0	-1/2	
1/2	0	-1/2	
-1/2	0	1/2	
0	1/2	1/2	
1	1/2	-1/2	
1	1/2	-1/2	
0	1/2	1/2	

1.	1/2	0	1/2	
2.	0	1/2	1/2	→ (#12)

1b → 2d ✓

Similarly, Wyckoff position splitting of Ba2, Na2, P1, O1 and O2 atoms and their corresponding atomic orbits in subgroup unit cell are found by repeating the same calculations. After calculations are completed, it is proved that all results match up with expected results in this case.

4. Calculating Degree of Lattice Distortion

Strain that results in lattice distortion in crystals is discussed in Section 7.4. Distortion between reference structure of #12 in crystallography database and actual glaserite-type structure of #12 will be found.

The following relation gives degree of lattice distortion [24];

$$S = \frac{1}{3} \sqrt{\sum_{i=1}^3 \eta_i^2}$$

η_i represent eigenvalues of finite Lagrangian strain tensor.

$$\boldsymbol{\eta} = \frac{1}{2}(e + e^T + e^T e) \text{ and } e = R_2 R_1^{-1} - I$$

In order to find degree of lattice distortion, metric tensors and standard root tensors of the two structures will be found first.

Lattice parameters of cell number 1 (undeformed):

9.7289 5.6170 7.2600 90.000 90.000 90.000

Lattice parameters of cell number 2 (deformed):

9.7430 5.6220 7.2600 90.000 90.100 90.000

First cell corresponds to ideal structure and second one represents deformed (distorted) parameters of GTS.

Let G_1 and G_2 be the corresponding metric tensors. Using lattice parameters, metric tensors and standard root tensors are found.

$$G_1 = \begin{pmatrix} 94.65208 & 0 & 0 \\ 0 & 31.55069 & 0 \\ -0.12345 & 0 & 52.70760 \end{pmatrix}$$

$$G_2 = \begin{pmatrix} 94.92605 & 0 & -0.12345 \\ 0 & 31.60688 & 0 \\ -0.12345 & 0 & 52.70760 \end{pmatrix}$$

Standard root tensors;

$$R_1 = \begin{pmatrix} 9.72893 & 0 & 0 \\ 0 & 5.61700 & 0 \\ 0 & 0 & 7.26000 \end{pmatrix} \quad R_2 = \begin{pmatrix} 9.74300 & 0 & 0 \\ 0 & 5.62200 & 0 \\ 0 & 0 & 7.26000 \end{pmatrix}$$

Then, finite Lagrangian strain tensor and its eigenvalues are obtained by using GNU Octave [28].

```
>> e=R2*inv(R1)-I
e =

    0.0014459    0.0000000   -0.0010001
    0.0000000    0.0008902    0.0000000
   -0.0007463    0.0000000   -0.0000005

>> n=1/2*(e+transpose(e)+transpose(e)*e)
n =

    0.0014472    0.0000000   -0.0008739
    0.0000000    0.0008906    0.0000000
   -0.0008739    0.0000000   -0.0000000

>> eigenvalue=eig(n)
eigenvalue =

   -0.00041100
    0.00089055
    0.00185825
```

$$\eta_1 = -0.00041100 \quad \eta_2 = 0.00089055 \quad \eta_3 = 0.00185825$$

$$S = \frac{1}{3} \sqrt{\eta_1^2 + \eta_2^2 + \eta_3^2}$$

From calculation, degree of lattice distortion between two structures is found as;

$$S = 0.00070040 \cong 0.0007$$

Strain result is compatible with the STRUCTURE RELATIONS program's results.

5. Calculating Degree of Global Distortion

Global distortion amplitude is calculated by displacements and corresponding site's multiplicities. Global distortion gives information of atomic displacement between reference structure and GTS.

WP		Atom	Atomic Displacements			
			u_x	u_y	u_z	$ u $
2b	(0,1/2,0)	Na1	0.0000	0.0000	0.0000	0.0000
2d	(0,1/2,1/2)	Ba1	0.0000	0.0000	0.0000	0.0000
4i	(x,0,z)	Ba2	0.0001	0.0000	0.0002	0.0019
4i	(x,0,z)	P1	0.0008	0.0000	-0.0003	0.0078
4i	(x,0,z)	O1	-0.0020	0.0000	0.0063	0.0499
4i	(x,0,z)	O2	0.0012	0.0000	-0.0039	0.0307
8j	(x,y,z)	O2_2	-0.0011	-0.0011	0.0010	0.0144

Figure 7.12. Atomic Displacements between Reference Structure and Glaserite-type Structure

Maximum distance between the atomic positions of the structures is:

$$d_{\max} = 0.0499$$

u_x, u_y and u_z are given in relative units and $|u|$ represents absolute distance in Å.

Let n be number of atoms and m be corresponding site's symmetry.

Global distortion amplitude is found by the following formula:

$$\sqrt{\sum_{i=1}^n u_i^2 m_i}$$

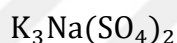
From STRUCTURE RELATIONS program, global distortion amplitude is found 0.0884 for this case.

III. APPLICATION OF GROUP THEORY TO THE GLASERITE-TYPE STRUCTURES FAMILY

8. INTRODUCTION TO GLASERITE AND GLASERITE-TYPE COMPOUNDS

Glaserite is a mineral that can be found naturally as shells in fumaroles of volcanoes and as components in oceanic, lacustrine and continental evaporite deposits which was firstly determined in 1928 by Gossner. Glaserite is also called Aphthitalite having the unchangeable and salt meaning in Greek [30]. Glaserite is in trigonal crystal system and belongs to $P - 3m1$ (#164) space group.

Formula of the glaserite is [31]:



Glaserite-like or glaserite-type compounds (GTC) refer to the minerals and synthetic substances which have isostructural properties with glaserite. Hexagonal arrangement of the cations and anions of the glaserite is formed in two types of columns (see Figure 8.1). First type of columns contains only cations (K^+ and Na^+) while second type contains both anions and cations (K^+ and SO_4^{2-}). Glaserite structure has been examined as hexagonal packing, as seen in Figure 8.2, composed of rods which anions and cations are tightly bound along it. This arrangement may be different for glaserite-type compounds since they have similarity to the glaserite but they are not necessarily identical to it. Making an analogy between the ions of glaserite and GTCs can require to determine the vacancies of the GTC ions along the columns [21] [32] [33] [34].

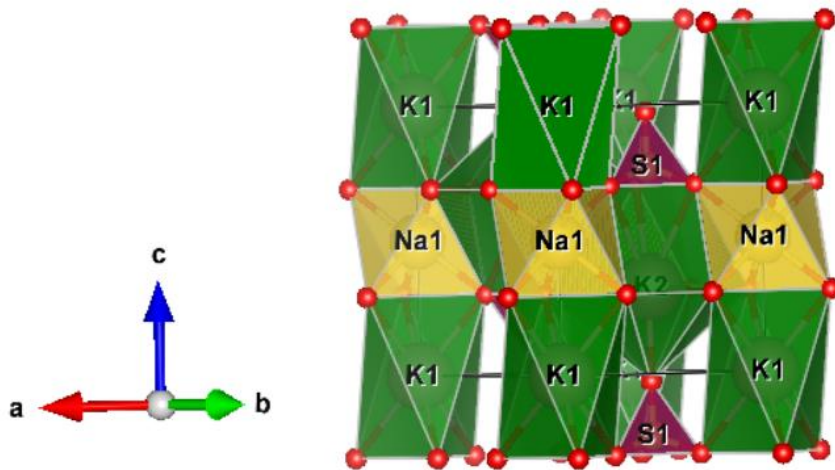


Figure 8.1. Hexagonal Packing Composed of Two Types of Columns [26]

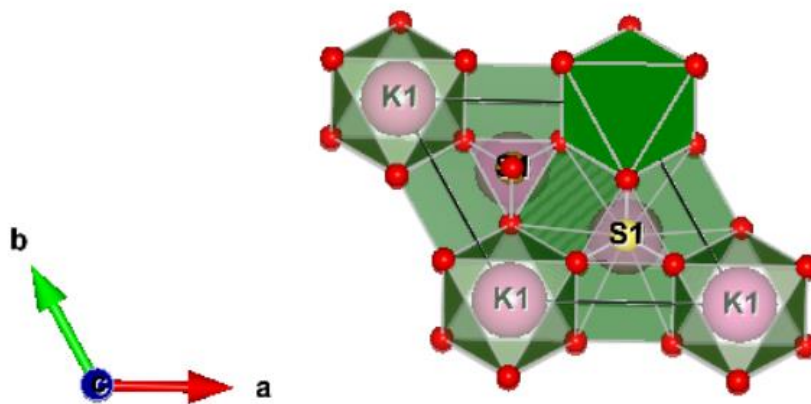
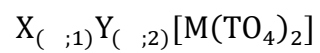


Figure 8.2. Hexagonal Arrangement of the Glaserite [26]

General formula of the GTC structure is figured out as follows [21]:



This formula gives information of two significant structural properties about glaserite-type compounds [21]:

1. $\infty[\text{M}(\text{TO}_4)_2]$ layer is the main structural unit and all atomic positions are fully occupied on this layer.
2. Occupancy of X and Y atomic positions are related to layer charge. Either both of them may be occupied; one is occupied while the other one unoccupied; or both of them may be unoccupied.
3. X and Y positions are not occupied when the layers of GTC are electroneutral. $\text{Ni}(\text{ReO}_4)_2$ and $\text{Zr}(\text{MoO}_4)_2$ are examples of this condition.



9. CLASSIFICATION OF KNOWN GLASERITE-TYPE COMPOUNDS

Stability condition of glaserite-type topology was defined in 1996 as [35];

$$0.59 < \Delta r < 0.89$$

where Δr is Shannon ionic radii and $\Delta r(\text{\AA}) = r_X(Y) - r_M$.

After study and revision of the GTC by Nikolova and Kostov-Kytin [21], considering the structures of Tl_2WO_4 and $\text{CsAl}(\text{MoO}_4)_2$, stability condition is expanded as;

$$0 < \Delta r < 1.345$$

Crystal characterization of over 100 GTC with glaserite-type topology (GTT) which was studied in this thesis was collected by Nikolova and Kostov-Kytin of the Institute of Mineralogy and Crystallography, Bulgarian Academy of Sciences. Except one compound, all of them are oxides. Nikolova and Kostov-Kytin evaluated chemical diversity and structural versatility of the GTT. Stability criteria was outlined with respect to the cation compositions and site occupancy by them [21] [34] [36] [37].

According to the revisions and verifications of gathered GTCs up to now reconsidered by Nikolova and Kostov-Kytin, information on glaserite-type compounds and topology is summarized as below:

“

1. There are 5 minerals and more than 100 synthetic compounds that adopt glaserite-type topology.
2. From general formula, X, Y, M and T cations correspond 47 elements of the periodic table.
3. T position is substituted by 11 elements consisting of transition metals (V, Cr, Mo, W, Re, Fe, Ru) and non-metals (Si, P, S, Se). T is always fully occupied.

4. M position is substituted by 32 elements consisting of alkali metal (Na), alkali earth metals (Mg, Ca), transition metals (Sc, Y, Ti, Zr, Hf, V, Cr, Mo, Mn, Fe, Co, Ni, Cu, Zn, Cd), lanthanides (Gd, Tb, Dy, Ho, Er, Tm, Yb, Lu) and poor metals (Al, In, Tl, Ge, Sn, Sb). Like T position, M is also fully occupied.
5. X and Y are substituted by 10 elements. When they are occupied, they consist of alkali metals (Na, K, Rb, Cs), alkali earth metals (Ca, Sr, Ba), transition metals (Ag) and poor metals (Tl, Pb).
6. The charge of ${}^2[M(\text{TO}_4)_2]$ layer takes one of the 0, -1, -2, -3, -4, -6 values." [21]

Considering number of elements occupying the atomic position; X and Y positions may have 0; 1 and 2 elements while M and T cation positions may have 1 and 2 elements.

Table 9.1. Derivatives of the General Formula of GTC [21]

No	General Formula	Conditions	Example	Number of GTC
1	$\text{XY}_2[\text{M}(\text{TO}_4)_2]$	$\text{X} \neq \text{Y} \neq \text{M} \neq \text{T}$	$\text{BaNa}_2\text{Mg}(\text{PO}_4)_2$	12
2	$\text{XY}_2[\text{M}(\text{TO}_4)_2]$	$\text{X} = \text{Y} \neq \text{M} \neq \text{T}$	$\text{Ag}_3\text{Fe}(\text{VO}_4)_2$	31
3	$\text{XY}_2[\text{M}(\text{TO}_4)_2]$	$\text{X} \neq \text{Y}; \text{X} = \text{M}; \text{Y} \neq \text{M} \neq \text{T}$	KNaSO_4	1
4	$\text{XY}_\square[\text{M}(\text{TO}_4)_2]$	$\text{X} \neq \text{M} \neq \text{T}; \text{Y} = 0$	$\text{RbFe}(\text{MoO}_4)_2$	41
5	$(\text{X}_1, \text{X}_2)\text{Y}_\square[\text{M}(\text{TO}_4)_2]$	$\text{X}_1 \neq \text{X}_2 \neq \text{M} \neq \text{T}; \text{Y} = 0$	$\text{Ba}_{0.3}\text{Sr}_{0.7}\text{Zr}(\text{PO}_4)_2$	1
6	$\text{X}(\text{Y}_1, \text{Y}_2)[\text{M}(\text{TO}_4)_2]$	$\text{X} = \text{Y}_1 \neq \text{Y}_2; \text{Y}_2 = \text{M} \neq \text{T}$	BaNaPO_4	4
7	$\text{X}_\square\text{Y}_2[\text{M}(\text{TO}_4)_2]$	$\text{Y} \neq \text{M} \neq \text{T}; \text{X} = 0$	$\text{K}_2\text{Zr}(\text{PO}_4)_2$	1
8	$\text{X}_\square\text{Y}_\square[\text{M}(\text{TO}_4)_2]$	$\text{M} \neq \text{T}; \text{X} = 0, \text{Y} = 0$	$\text{Ni}(\text{ReO}_4)_2$	7
9	$\text{X}_\square\text{Y}_\square[\text{M}(\text{T}_1, \text{T}_2)\text{O}_4)_2]$	$\text{M} \neq \text{T}_1; \text{T}_1 \neq \text{T}_2; \text{X} = 0, \text{Y} = 0$	$\text{Zr}((\text{Mo}, \text{W})\text{O}_4)_2$	1
10	$\text{X}_\square\text{Y}_\square[(\text{M}_1, \text{M}_2)(\text{TO}_4)_2]$	$\text{X} \neq \text{M}_1 \neq \text{M}_2 \neq \text{T}; \text{Y} = 0$	$\text{K}(\text{Mg}_{0.5}\text{Zr}_{0.5})(\text{MoO}_4)_2$	1
11	$\text{XY}_2[\text{M}(\text{TO}_4)_2]$	$\text{X} = \text{Y} = \text{M} \neq \text{T}$	Tl_2WO_4	2
12	$\text{XY}_2\text{H}[\text{M}(\text{TO}_4)_2]$	$\text{X} = \text{Y} \neq \text{M} \neq \text{T}$	$\text{Na}_3\text{HMg}(\text{PO}_4)_2$	5
13	$\text{XY}_\square\text{H}[\text{M}(\text{TO}_4)_2]$	$\text{X} \neq \text{M} \neq \text{T}; \text{Y} = 0$	$\text{KHZr}(\text{PO}_4)_2$	2

Table 9.1 (obtained by Nikolova and Kostov-Kytin, *Bulgarian Chemical Communications, Volume 45, Number 4, pp. 418–426, 2013*) shows structural diversity of GTC with respect to the specifications and occupancy of the positions of cations and corresponding examples.



10. IDENTIFICATION OF RELATIONS OF GLASERITE-TYPE SUB-FAMILIES

Determined group-subgroup relations are identified via transformation matrix, index, maximum distance between the atomic positions of the paired atoms, the degree of lattice distortion (spontaneous strain), the measure of compatibility (measure of similarity) and the global distortion on the following table [38] [39] [24]. Between the structures of the same space groups (with index 1), “high symmetry” and “low symmetry” labels shows transformation direction since there can be no actual high and low symmetry hierarchy between them.

The structures data are available from:

http://yunus.hacettepe.edu.tr/~emre.tasci/strrel_serpil_albay_glaserites_case_study/all_structure_data.html address, where they can also be visualized directly or downloaded in CIF format.

Alternative link:

http://test3.cryst.ehu.es/strrel_serpil_albay_glaserites_case_study/all_structure_data.html

Table 10.1. Relations of Glaserite-type Sub-Families

High Symmetry Structure			Low Symmetry Structure								
ID	Space Group	Formula	ID	Space Group	Formula	Index	Transformation Matrix (P)	Max. Distance (d _{max}) (Å)	Degree of Lattice Distortion (S)	Measure of Compatibility (Δ)	Global Distortion (Å)
19	P-3m1(#164)	RbFe(MoO4)2	20	P-3(#147)	RbFe(MoO4)2	2	a,b,c;0,0,0	0.3226	0.0069	0.067	0.7943
19	P-3m1(#164)	RbFe(MoO4)2	22	P-3(#147)	CsFe(SO4)2	2	a,b,c;0,0,0	1.0558	0.0933	0.495	2.0429
98	P-3m1(#164)	BaZr(PO4)2	96	C2/m(#12)	BaGe(PO4)2	3	a-b,a+b,c;0,0,-1/2	0.9691	0.0565	0.339	1.8982
5	P-3m1(#164)	RbIn(WO4)2	20	P-3(#147)	RbFe(MoO4)2	2	a,b,c;0,0,0	0.4002	0.0223	0.096	1.06
7	P-3m1(#164)	KSc(MoO4)2	8	P-3c1(#165)	KFe(MoO4)2	2	a,b,2c;0,0,0	0.1976	0.0107	0.032	0.7437
6	P-3m1(#164)	KAl(MoO4)2	8	P-3c1(#165)	KFe(MoO4)2	2	a,b,2c;0,0,0	0.2145	0.0098	0.038	0.769
52	C2/m(#12)	NaFe(SeO4)2	65	C2/c(#15)	NaFe(MoO4)2	2	a,-b,-2c;0,0,0	1.3166	0.0559	0.757	4.2437
51	C2/m(#12)	NaV(SO4)2	65	C2/c(#15)	NaFe(MoO4)2	2	a,-b,-2c;0,0,0	1.2632	0.0605	0.746	4.0584
58	C2/m(#12)	NaFe(SO4)2	65	C2/c(#15)	NaFe(MoO4)2	2	a,-b,-2c;0,0,0	1.239	0.06	0.724	4.1439
58	C2/m(#12)	NaFe(SO4)2	67	C2/c(#15)	NaAl(MoO4)2	2	a,-b,-2c;0,0,0	1.0902	0.0596	0.656	3.7387
98	P-3m1(#164)	BaZr(PO4)2	60	C2/m(#12)	BaHf(PO4)2	3	a-b,a+b,c;0,0,-1/2	0.9263	0.0251	0.218	1.654
98	P-3m1(#164)	BaZr(PO4)2	61	C2/m(#12)	BaSn(PO4)2	3	a-b,a+b,c;0,0,0	1.0312	0.0417	0.333	1.9909
119	P-3m1(#164)	KFe(MoO4)2	116	P-3c1(#165)	KIn(WO4)2	2	a,b,2c;0,0,0	1.9289	0.0114	0.21	8.0092
119	P-3m1(#164)	KFe(MoO4)2	8	P-3c1(#165)	KFe(MoO4)2	2	a,b,2c ; 0,0,1/2	0.1933	0.0009	0.028	0.6742

8	P-3c1(#165)	KFe(MoO4)2	67	C2/c(#15)	NaAl(MoO4)2	3	a-b,-a-b,-c ; 0,0,0	0.5625	0.0361	0.195	2.036
57	C2/m(#12)	BaZr(PO4)2	70	C2/c(#15)	PbTi(PO4)2	2	a+2c,-b,-a ; 1/4,1/4,-1/2	0.3891	0.0256	0.084	1.0493
116	P-3c1(#165)	KIn(WO4)2	201	P2/c(#13)	NaHZr(PO4)2	6	a-b,a+b,-a+b+c ; - 1/2,0,0	1.2322	0.0661	0.183	4.109
116	P-3c1(#165)	KIn(WO4)2	116_1	C2/c(#15)	KIn(WO4)2	3	a-b,a+b,-a+b+c ; - 1/2,0,0				
116_1	C2/c(#15)	KIn(WO4)2	201	P2/c(#13)	NaHZr(PO4)2	2	-a,b,-c;-1/2,0,0	1.2322	0.0661	0.21	4.6764
10	P-3m1(#164)	RbIn(MoO4)2	20	P-3(#147)	RbFe(MoO4)2	2	a,b,c ; 0,0,0	0.3547	0.0208	0.083	0.9284
57	C2/m(#12)	BaZr(PO4)2	201	P2/c(#13)	NaHZr(PO4)2	4	a,-b,-a-2c ; 3/4,1/4,-1/2	1.4236	0.036	0.325	6.3346
57	C2/m(#12)	BaZr(PO4)2	57_1	C2/c(#15)	BaZr(PO4)2	2	a,-b,-a-2c ; 3/4,1/4,-1/2				
57_1	BaZr(PO4)2	C2/c(#15)	201	P2/c(#13)	NaHZr(PO4)2	2	-a,b,-c;-1/2,0,0	1.4236	0.036	0.325	6.3346
98	P-3m1(#164)	BaZr(PO4)2	22	P-3(#147)	CsFe(SO4)2	2	a,b,c ; 0,0,1/2	0.7021	0.0476	0.308	1.7074
99	C2/c(#15)	SrTi(PO4)2	200	P2/c(#13)	KHZr(PO4)2	2	-a,b,-c ; 0,0,0	2.238	0.4419	7.51	11.0826
67	C2/c(#15)	NaAl(MoO4)2	200	P2/c(#13)	KHZr(PO4)2	2	-c,b,a+c ; 1/4,3/4,0	2.5205	0.2082	1.566	11.4488
134	P-3m1(#164)	CsEr(WO4)2	116	P-3c1(#165)	KIn(WO4)2	2	a,b,2c ; 0,0,0	0.4806	0.0482	0.169	1.7369
136	P-3m1(#164)	CsLu(WO4)2	49	C2/m(#12)	KFe(CrO4)2	3	a-b,a+b,c ; 0,0,-1/2	1.0446	0.0845	0.343	2.0722
47	C2/m(#12)	KFe(SO4)2	65	C2/c(#15)	NaFe(MoO4)2	2	-a,b,-2c ; 0,0,0	2.241	0.0811	1.049	7.6555
100	C2/m(#12)	NaCr(CrO4)2	201	P2/c(#13)	NaHZr(PO4)2	4	a,-b,-a-2c ; 3/4,1/4,0	1.3196	0.0326	0.242	5.8411
137	P-3m1(#164)	CsYb(WO4)2	102	C2/m(#12)	RbCr(CrO4)2	3	a-b,a+b,c ; 0,0,-1/2	1.0089	0.087	0.399	2.1043
53	C2/m(#12)	BaMo(PO4)2	65	C2/c(#15)	NaFe(MoO4)2	2	-a,b,-2c ; 0,0,0	2.066	0.0768	0.974	6.6461
134	P-3m1(#164)	CsEr(WO4)2	100	C2/m(#12)	NaCr(CrO4)2	3	a-b,a+b,c ; 0,0,-1/2	0.9109	0.1157	0.228	1.8962

121	P-3m1(#164)	CsV(MoO4)2	96	C2/m(#12)	BaGe(PO4)2	3	a-b,a+b,c ; 0,0,-1/2	0.8988	0.1023	0.422	1.8108
32	P-3m1(#164)	K3Na(SeO4)2	31	P-3(#147)	K3Na(SeO4)2	2	a,b,c;0,0,0	0.0252	0.0033	0.003	0.0572
32	P-3m1(#164)	K3Na(SeO4)2	33	C2/c(#15)	K3Na(SeO4)2	6	a-b,-a-b,-2c ; 0,0,0	0.1906	0.0036	0.025	0.7001
32	P-3m1(#164)	K3Na(SeO4)2	32_1	C2/m(#12)	K3Na(SeO4)2	3	a-b,-a-b,-c ; 0,0,0				
32_1	C2/m(#12)	K3Na(SeO4)2	33	C2/c(#15)	K3Na(SeO4)2	2	-a,b,-2c ; 0,0,0	0.1906	0.0036	0.025	0.7001
75	P-3m1(#164)	K3Na(RuO4)2	74	C2/c(#15)	K3Na(RuO4)2	6	a-b,a+b,2c ; 0,0,1/2	0.3937	0.0046	0.055	1.3643
75	P-3m1(#164)	K3Na(RuO4)2	75_1	C2/m(#12)	K3Na(RuO4)2	3	a-b,a+b,c ; 0,0,1/2				
75_1	C2/m(#12)	K3Na(RuO4)2	74	C2/c(#15)	K3Na(RuO4)2	2	-a,b,2c;0,0,0	0.3937	0.0046	0.055	1.3643
28	P-3m1(#164)	K3Na(FeO4)2	48	C2/m(#12)	K3CaH(PO4)2	3	a-b,a+b,c ; 0,0,-1/2	0.5156	0.0215	0.047	0.9321
76	P-3m1(#164)	Rb3Na(RuO4) 2	48	C2/m(#12)	K3CaH(PO4)2	3	a-b,-a-b,-c ; 0,0,0	0.5528	0.0431	0.051	1.0369
48	C2/m(#12)	K3CaH(PO4)2	38	P2_1/m (#11)	Na3In(PO4)2	2	-a,b,-c ; -1/4,1/4,0	1.1719	0.0603	0.323	3.9408
59	C2/m(#12)	Ag3In(PO4)2	38	P2_1/m (#11)	Na3In(PO4)2	2	-a,-b,c ; 1/4,1/4,1/2	0.7441	0.0231	0.13	2.7218
38	P2_1/m (#11)	Na3In(PO4)2	171	P2_1/c (#14)	Na2SrMg(PO4)2	2	-a,b,-2c ; -1/2,0,0	2.1762	0.0258	0.493	11.4356
68	C2/c(#15)	Ag2SrMn(VO 4)2	171	P2_1/c (#14)	Na2SrMg(PO4)2	2	-a,b,-c ; 1/4,1/4,- 1/2	0.4262	0.0313	0.09	1.8956
2	C2/m(#12)	K2CsHo(PO4) 2	68	C2/c(#15)	Ag2SrMn(VO4) 2	2	-a,-b,2c ; 0,0,0	0.6342	0.06	0.25	2.6095
24	P-3m1(#164)	BaNa(PO4)2	34	C2/m(#12)	BaNa(PO4)2	3	a-b,-a-b,-c ; 1/2,- 1/2,0	0.0499	0.0007	0.005	0.0884
2	C2/m(#12)	BaNa(PO4)2	197	C2/c(#15)	K2KNa(CrO4)2	2	-a,b,-2c ; 0,0,0	0.6819	0.0306	0.159	2.2275
91	P-3m1(#164)	Na2CaMg(PO 4)2	2	C2/m(#12)	K2CsHo(PO4)2	3	a-b,a+b,c ; 0,0,-1/2	0.4599	0.0328	0.149	0.9404
197	C2/c(#15)	K2KNa(CrO4) 2	42	P2_1/c (#14)	Na2CaMg(PO4) 2	2	-a,b,-c ; -1/4,1/4,- 1/2	2.2357	0.0731	0.206	8.7642

59	C2/m(#12)	Ag3In(PO4)2	78	C2/c(#15)	K3Na(MoO4)2	2	-a,b,-2c ; 0,0,0	1.195	0.061	0.376	4.4172
118	P-3m1(#164)	KNa(SO4)	29	P3m1 (#156)	(K, Na)3Na(SO4)2	2	b,a,-c ; 2/3,1/3,0.00379	3.2411	0.0062	0.356	7.1515
38	P2_1/m (#11)	Na3In(PO4)2	37	P-1(#2)	Na3HZr(SiO4)2	2	a,b,c;0,0,0	0.4854	0.0191	0.149	1.5782
26	P-3m1(#164)	K3V(VO4)2	30	P-3(#147)	Ag2BaMn(VO4) 2	2	a,b,c;0,0,0	0.4689	0.0089	0.06	1.2048
117	P-3m1(#164)	K2RbGd(VO4) 2	93	P-3(#147)	K2CsSc(PO4)2	2	a,b,c;0,0,0	0.5169	0.0445	0.163	1.0519
123	P-3m1(#164)	K2CsYb(PO4) 2	170	P-3(#147)	Na2BaMg(PO4) 2	2	-a,-b,c ; 0,0,0	0.5107	0.059	0.16	1.1898
28	P-3m1(#164)	K3Na(FeO4)2	72	P-3(#147)	K3Sc(PO4)2	6	a-b,a+2b,c ; 0,0,0	0.6505	0.035	0.156	2.8182
28	P-3m1(#164)	K3Na(FeO4)2	28_1	P-31m (#162)	K3Na(FeO4)2	3	a-b,a+2b,c ; 0,0,0				
28_1	P-31m (#162)	K3Na(FeO4)2	72	P-3(#147)	K3Sc(PO4)2	2	a,b,c;0,0,0	0.6505	0.035	0.156	2.8182
87	C2/c(#15)	(K2.5Na0.5)Na a(MoO4)2	63	P2_1/c (#14)	Sr3Mg(SiO4)2	2	a+c,-b,-c ; 3/4,1/4,1/2	2.6475	0.0569	0.297	11.3791
170	P-3(#147)	Na2BaMg(PO4) 2	128	P-1(#2)	Na3MgH(PO4)2	3	a,b,c;0,0,0	3.411	0.3161	0.435	6.8378
59	C2/m(#12)	Ag3In(PO4)2	64	C2/c(#15)	Na3Fe(PO4)2	2	-a,b,-2c ; 0,0,0	1.7314	0.0413	0.452	6.5336
129	P-3m1(#164)	K2RbTb(VO4) 2	93	P-3(#147)	K2CsSc(PO4)2	2	a,b,c;0,0,0	0.524	0.044	0.16	1.0646
65	C2/c(#15)	NaFe(MoO4)2	67	C2/c(#15)	NaAl(MoO4)2	1	-a,b,-c;0,0,-1/2	0.2467	0.0142	0.05	0.7617
5	P-3m1(#164)	RbIn(WO4)2	10	P-3m1(#164)	RbIn(MoO4)2	1	a,b,c;0,0,0	0.1532	0.0022	0.028	0.384
6	P-3m1(#164)	KAl(MoO4)2	7	P-3m1(#164)	KSc(MoO4)2	1	a,b,c;0,0,0	0.2137	0.0195	0.044	0.4723
57	C2/m(#12)	BaZr(PO4)2	96	C2/m(#12)	BaGe(PO4)2	1	-a,b,-c;0,0,0	0.2701	0.034	0.107	0.5736
5	P-3m1(#164)	RbIn(WO4)2	19	P-3m1(#164)	RbFe(MoO4)2	1	a,b,c;0,0,0	0.2622	0.015	0.049	0.7204
10	P-3m1(#164)	RbIn(MoO4)2	19	P-3m1(#164)	RbFe(MoO4)2	1	a,b,c;0,0,0	0.176	0.0136	0.03	0.4785

47	C2/m(#12)	KFe(SO4)2	49	C2/m(#12)	KFe(CrO4)2	1	-a,b,-c;0,0,-1/2	0.1808	0.0294	0.109	0.4171
20	P-3(#147)	RbFe(MoO4)2	22	P-3(#147)	CsFe(SO4)2	1	a,b,c;0,0,0	0.9942	0.0869	0.53	2.4021
51	C2/m(#12)	NaV(SO4)2	52	C2/m(#12)	NaFe(SeO4)2	1	-a,b,-c;0,0,0	0.1635	0.0182	0.023	0.3965
60	C2/m(#12)	BaHf(PO4)2	61	C2/m(#12)	BaSn(PO4)2	1	-a,b,-c;0,0,-1/2	0.3734	0.0153	0.113	0.7771
70	C2/c(#15)	PbTi(PO4)2	99	C2/c(#15)	SrTi(PO4)2	1	-a,b,-c;-1/2,0,-1/2	0.1033	0.0061	0.022	0.2768
119	P-3m1(#164)	KFe(MoO4)2	121	P-3m1(#164)	CsV(MoO4)2	1	a,b,c;0,0,0	0.4435	0.0332	0.156	0.8116
121	P-3m1(#164)	CsV(MoO4)2	124	P-3m1(#164)	CsAl(MoO4)2	1	a,b,c;0,0,0	0.0699	0.0098	0.04	0.2154
12	P-3m1(#164)	TlSc(MoO4)2	16	P-3m1(#164)	TlAl(MoO4)2	1	a,b,c;0,0,0	0.1663	0.021	0.059	0.4664
53	C2/m(#12)	BaMo(PO4)2	57	C2/m(#12)	BaZr(PO4)2	1	-a,b,-c ; 0,0,-1/2	0.2177	0.0157	0.09	0.4411
201	P2/c(#13)	NaHZr(PO4)2	200	P2/c(#13)	KHZr(PO4)2	1	-a,b,-c ; 0,0,-1/2	0.6374	0.0205	0.117	2.9392
61	C2/m(#12)	BaSn(PO4)2	96	C2/m(#12)	BaGe(PO4)2	1	-a,b,-c ; 0,0,-1/2	0.106	0.0187	0.016	0.2302
7	P-3m1(#164)	KSc(MoO4)2	12	P-3m1(#164)	TlSc(MoO4)2	1	-a,-b,c ; 0,0,0	0.1571	0.01	0.047	0.3342
52	C2/m(#12)	NaFe(SeO4)2	58	C2/m(#12)	NaFe(SO4)2	1	-a,b,-c ; 0,0,0	0.3527	0.0209	0.051	0.7342
19	P-3m1(#164)	RbFe(MoO4)2	135	P-3m1(#164)	CsTm(WO4)2	1	a,b,c;0,0,0	0.0524	0.035	0.048	0.1455
135	P-3m1(#164)	CsTm(WO4)2	98	P-3m1(#164)	BaZr(PO4)2	1	a,b,c ; 0,0,1/2	0.2712	0.0743	0.138	0.6054
98	P-3m1(#164)	BaZr(PO4)2	136	P-3m1(#164)	CsLu(WO4)2	1	a,b,c ; 0,0,1/2	0.2826	0.0561	0.139	0.6619
47	C2/m(#12)	KFe(SO4)2	101	C2/m(#12)	KCr(CrO4)2	1	-a,b,-c ; 0,0,-1/2	0.315	0.0269	0.104	0.5518
101	C2/m(#12)	KCr(CrO4)2	51	C2/m(#12)	NaV(SO4)2	1	-a,b,-c ; 0,0,-1/2	0.2103	0.0416	0.035	0.5052
102	C2/m(#12)	RbCr(CrO4)2	100	C2/m(#12)	NaCr(CrO4)2	1	-a,b,-c ; 0,0,0	0.4096	0.0653	0.178	0.8332
47	C2/m(#12)	KFe(SO4)2	52	C2/m(#12)	NaFe(SeO4)2	1	-a,b,-c ; 0,0,0	0.4556	0.0393	0.103	0.8144

16	P-3m1(#164)	TlAl(MoO4)2	10	P-3m1(#164)	RbIn(MoO4)2	1	-a,-b,c ; 0,0,0	0.2294	0.0238	0.054	0.6696
124	P-3m1(#164)	CsAl(MoO4)2	137	P-3m1(#164)	CsYb(WO4)2	1	a,b,c ; 0,0,1/2	0.3778	0.0314	0.091	0.7448
32	P-3m1(#164)	K3Na(Se4)2	10	P-3m1(#164)	RbIn(MoO4)2	1	a,b,c;0,0,0	0.3766	0.0079	0.091	0.99
33	C2/c(#15)	K3Na(SeO4)2	65	C2/c(#15)	NaFe(MoO4)2	1	-a,b,-c ; 0,0,-1/2	0.6739	0.0536	0.248	2.2289
75	P-3m1(#164)	K3Na(RuO4)2	32	P-3m1(#164)	K3Na(SeO4)2	1	-a,-b,c ; 0,0,1/2	0.1284	0.0107	0.016	0.3063
76	P-3m1(#164)	Rb3Na(RuO4) 2	75	P-3m1(#164)	K3Na(RuO4)2	1	a,b,c;0,0,0	0.0415	0.0106	0.023	0.0977
76	P-3m1(#164)	Rb3Na(RuO4) 2	28	P-3m1(#164)	K3Na(FeO4)2	1	-a,-b,c ; 0,0,1/2	0.0778	0.0254	0.016	0.2215
28	P-3m1(#164)	K3Na(FeO4)2	25	P-3m1(#164)	K3Na(CrO4)2	1	-a,-b,c ; 0,0,1/2	0.0333	0.0026	0.013	0.0864
48	C2/m(#12)	K3CaH(PO4)2	35	C2/m(#12)	Na3HZr(GeO4)2	2	-a,b,-2c ; -1/2,0,0	2.1519	0.0327	0.2203	6.8425
33	C2/c(#15)	K3Na(SeO4)2	68	C2/c(#15)	Ag2SrMn(VO4) 2	1	-a,-b,c ; 0,0,0	0.4735	0.0367	0.091	1.5825
74	C2/c(#15)	K3Na(RuO4)2	68	C2/c(#15)	Ag2SrMn(VO4) 2	1	-a,b,-c ; 0,0,-1/2	1.7163	0.0481	0.204	5.6279
68	C2/c(#15)	Ag2SrMn(VO 4)2	71	C2/c(#15)	Na2BaCu(VO4) 2	1	-a,b,-c ; 0,0,-1/2	0.4411	0.0144	0.137	1.3198
171	P2_1/c (#14)	Na2SrMg(PO 4)2	42	P2_1/c (#14)	Na2CaMg(PO4) 2	1	-a,b,-c ; -1/2,1/2,- 1/2	0.369	0.0069	0.067	1.7079
42	P2_1/c (#14)	Na2CaMg(PO 4)2	44	P2_1/c (#14)	Ca3Mg(SiO4)2	1	a+c,-b,-c ; 0,0,-1/2	0.3906	0.0108	0.063	1.5575
44	P2_1/c (#14)	Ca3Mg(SiO4) 2	63	P2_1/c (#14)	Sr3Mg(SiO4)2	1	-a,b,-c ; 0,1/2,-1/2	0.7056	0.0196	0.088	2.7615
2	C2/m(#12)	K2CsHo(PO4) 2	34	C2/m(#12)	BaNa(PO4)2	1	-a,b,-c ; -1/2,0,0	0.7275	0.0407	0.191	1.617
24	P-3m1(#164)	BaNa(PO4)2	118	P-3m1(#164)	KNa(SO4)	1	-a,-b,c ; 0,0,1/2	0.2927	0.0032	0.027	0.5525
91	P-3m1(#164)	Na2CaMg(PO 4)2	77	P-3m1(#164)	K2RbGd(VO4)2	1	a,b,c ; 0,0,1/2	0.4996	0.033	0.027	0.7781
78	C2/c(#15)	K3Na(MoO4) 2	80	C2/c(#15)	K3Na(WO4)2	1	-a,b,-c ; 0,0,-1/2	0.0496	0.0029	0.005	0.1729

80	C2/c(#15)	K3Na(WO4)2	64	C2/c(#15)	Na3Fe(PO4)2	1	-a,b,-c ; 0,0,-1/2	1.7022	0.102	0.176	5.4742
25	P-3m1(#164)	K3Na(CrO4)2	26	P-3m1(#164)	K3V(VO4)2	1	-a,-b,c ; 0,0,0	0.342	0.0186	0.065	0.9928
117	P-3m1(#164)	K2RbGd(VO4) 2	123	P-3m1(#164)	K2CsYb(PO4)2	1	a,b,c;0,0,0	0.4003	0.0324	0.139	0.8716
26	P-3m1(#164)	K3V(VO4)2	117	P-3m1(#164)	K2RbGd(VO4)2	1	-a,-b,c ; 0,0,1/2	0.1864	0.0283	0.032	0.4959
123	P-3m1(#164)	K2CsYb(PO4) 2	129	P-3m1(#164)	K2RbTb(VO4)2	1	a,b,c;0,0,0	0.3943	0.0289	0.136	0.8595
95	P-1(#2)	KMn(SeO4)2	37	P-1(#2)	Na3HZr(SiO4)2	2	2a,b,c ; 1/2,1/2,1/2	2.9086	0.1197	0.449	8.682
95	P-1(#2)	KMn(SeO4)2	128	P-1(#2)	Na3MgH(PO4)2	1	a,b,c;0,0,0	3.411	0.4433	0.795	5.8025
93	P-3(#147)	K2CsSc(PO4) 2	30	P-3(#147)	Ag2BaMn(VO4) 2	1	-a,-b,c ; 0,0,1/2	0.657	0.0317	0.214	1.7414
66	C2/c(#15)	Ag3Fe(VO4)2	197	C2/c(#15)	K2KNa(CrO4)2	1	-a,b,-c ; 0,0,-1/2	2.1632	0.044	0.301	6.2186
72	P-3(#147)	K3Sc(PO4)2	73	P-3(#147)	K3Lu(PO4)2	1	a,b,c;0,0,0	0.1658	0.0093	0.02	0.6182
73	P-3(#147)	K3Lu(PO4)2	126	P-3(#147)	Ba3Mg(SiO4)2	1	b,a,-c ; 0,0,0	0.5654	0.022	0.123	1.9609
31	P-3(#147)	K3Na(SeO4)2	126	P-3(#147)	Ba3Mg(SiO4)2	3	-a+b,-a-2b,c ; 0,0,0	0.323	0.0247	0.041	1.2264
31	P-3(#147)	K3Na(SeO4)2	20	P-3(#147)	RbFe(MoO4)2	1	a,b,c;0,0,0	0.4847	0.0241	0.126	1.2879
118	P-3m1(#164)	KNa(SO4)	122	P-3m1(#164)	Tl2(MoO4)	1	-a,-b,c ; 0,0,1/2	0.4517	0.0543	0.048	1.0458
122	P-3m1(#164)	Tl2(MoO4)	21	P-3m1(#164)	Tl2(WO4)	1	a,b,c;0,0,0	0.0728	0.0009	0.009	0.185
87	C2/c(#15)	(K2.5Na0.5) Na(MoO4)2	66	C2/c(#15)	Ag3Fe(VO4)2	1	-a,-b,c ; 0,0,-1/2	0.7987	0.0678	0.163	3.0329
128	P-1(#2)	Na3MgH(PO4) 2	37	P-1(#2)	Na3HZr(SiO4)2	2	2a,b,c ; 1/2,0,0	2.4789	0.1549	0.907	8.9617

11. CONCLUSION

Group-subgroup relations of Glaserite-type compounds were determined and corresponding transformations were shown on the diagram tree. Online version of the diagram can also be visited via:

http://yunus.hacettepe.edu.tr/~emre.tasci/strel_serpil_albay_glaserites_case_study/DiagramComplete_size.png

Alternative link:

http://test3.cryst.ehu.es/strel_serpil_albay_glaserites_case_study/DiagramComplete_size.png

Some of the structures' data collected by Nikolova and Kostov-Kytin was excluded due to duplication and the remaining ones are sorted in subclasses according to the structural diversity of the GTC as shown in Table 9.1. Making an analogy between the structures requires structural similarity by means of space groups' constraints. Lattice compatibility of two space groups that is validated by group theory is not the only constraints for comparison of two structure i.e., there must be Wyckoff splitting compatibility, also.

Resistance of the reformation of the new unit cell during transformation constitutes degree of lattice distortion. In this study, among the compared structures, transformation from the group $P-3m1$ (#164) to the subgroups $P-3$ (#147), $P-3c1$ (#165) and $C2/c$ (#15) constitutes bigger lattice distortion amplitude compared to other group-subgroup transitions.

Global distortion amplitude is calculated via low symmetry structure's sites' multiplicities and the corresponding atomic displacements between the high and low symmetry structures. According to the diagram tree, transition from high symmetry structure $\text{RbFe}(\text{MoO}_4)_2$ ($P-3m1$) to low symmetry structure $\text{RbFe}(\text{MoO}_4)_2$ ($P-3$) reveals the biggest global distortion amplitude (11.4488 Å). Three of the four results that have global distortion amplitude above 10 Å belong to $(P-3m1) \rightarrow (P-3)$ transformation (see Table 10.1).

Transformation of the structures that are divided into similar classification in accordance with their cations' occupancies gives more precise results. On the other hand, by assuming a void on an excess element provides the determination of group-subgroup relations between structures with different number of atoms in their compared unit cells. $K_3Na(SeO_4)_2$ crystal belongs to 2nd subclass, $XY_2[M(TO_4)_2]$, ($X = Y \neq M \neq T$) of the general formula $X_{(;1)}Y_{(;2)}[M(TO_4)_2]$ of GTC while $RbIn(MO_4)_2$ crystal in the form of 4th derivative $XY [M(TO_4)_2]$, ($X \neq M \neq T; Y = 0$) of the general formula. Both structures belong to same space group. Assuming the void on K_1 atom (2d WP) helps to relate these two structures with small strain and global distortion.

It is possible to estimate possible theoretical structures in intermediate group's setting between two space groups to find maximal subgroup and minimal supergroup. According to the diagram tree, there is a transformation between $K_3Na(SeO_4)_2$ ($P - 3m1$) and $K_3Na(SeO_4)_2$ $C2/c$ (#15) with index 6. There may be an intermediate group between them. By using online PSEUDO program [40][23] and after calculations, a possible structure $K_3Na(SeO_4)_2$ belonging to $C2/m$ (#12) space group is found. The other structures $KIn(WO_4)_2$ ($C2/c$ (#15)), $BaZr(PO_4)_2$ ($C2/c$ (#15)) and $K_3Na(RuO_4)_2$ ($C2/m$ (#12)) are possible estimated structures and are shown on Table 10.1 and the diagram.

Diagram tree shows all of the derived relations of group-subgroup containing transformation matrix, index, maximum distance between the atomic positions, the degree of lattice distortion, the measure of compatibility and the global distortion data. Moreover, big global distortions during phase transition are presented in color according to their range, possible theoretical structures are indicated via dashed lines and transformation of the structures by assumed voids are also distinguished by dashed and colored lines.

Since the calculation results take up a lot of space (around 270 pages in printed format), they are not included as hard copies in this thesis. The data output of

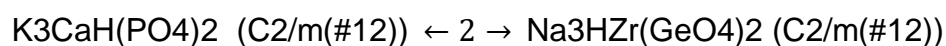
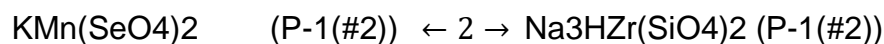
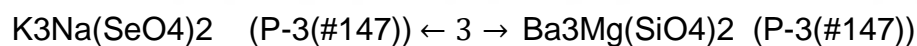
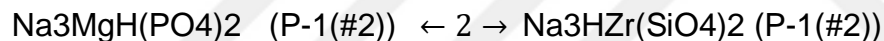
the relations of the pairs shown in diagram, along with other information, is accessible via the following link:

http://yunus.hacettepe.edu.tr/~emre.tasci/strrel_serpil_albay_glaserites_case_study/

Alternative link:

http://test3.cryst.ehu.es/strrel_serpil_albay_glaserites_case_study/

The relation between the structures of the same space groups generally has neither point group symmetry loss nor translational symmetry loss. According to the diagram, there are four cases of relations between the same space groups having a klassengleiche index, meaning that the volume of one of the unit cell is significantly different with respect to the others. The following four crystals' relations of the same space groups correspond to the transformation via klassengleiche index.



REFERENCES

- [1] A. Abney, A. Tyminski, and P. Nazarewicz, "Symmetry in Nature." [Online]. Available: http://jwilson.coe.uga.edu/EMT668/EMAT6680.2002.Fall/Nazarewicz/7210_final_2/7210_Project/. [Accessed: 10-Nov-2018].
- [2] T. Hahn and H. Wondratschek, *Symmetry of Crystals: Introduction to International Tables for Crystallography Vol. A*. Sofia: Heron Press, **1994**.
- [3] U. Müller, *Symmetry Relationships between Crystal Structures. Applications of Crystallographic Group Theory in Crystal Chemistry*. Oxford: Clarendon Press, **2012**.
- [4] G. G. Slabaugh, "Computing Euler angles from a rotation matrix," *Retrieved on August*, vol. 6, no. 2000, pp. 39–63, **1999**.
- [5] M. I. Aroyo *et al.*, "Bilbao Crystallographic Server: I. Databases and crystallographic computing programs," *Zeitschrift für Krist. Mater.*, vol. 221, no. 1, pp. 15–27, **2006**.
- [6] H. Arnold, "Transformations in Crsytallography," in *International Tables for Crystallography Volume A*, 5th ed., T. Hahn, Ed. Springer, **2005**.
- [7] H. Burzlaff, H. and Zimmerman, "Bases, Lattices, Bravais Lattices and Other Classifications," in *International Tables for Crystallography Volume A*, 5th ed., T. Hahn, Ed. Springer, pp. 742–749, **2005**.
- [8] M. I. Aroyo, A. Kirov, C. Capillas, J. M. Perez-Mato, and H. Wondratschek, "Bilbao Crystallographic Server. II. Representations of crystallographic point groups and space groups," *Acta Crystallogr. Sect. A Found. Crystallogr.*, vol. 62, no. 2, pp. 115–128, **2006**.
- [9] M. J. Buerger, *Introduction to crystal geometry*. New York: McGraw-Hill, **1971**.
- [10] M. M. Julian, *Foundations of Crystallography with Computer Applications*, 2nd ed. London: CRC Press, **2015**.
- [11] U. Müller, "Symmetry Relations between Crystal Structures.," in *Summer School on Mathematical and Theoretical Crystallography 27 April - 3 May*, **2008**.
- [12] M. De Graef, "A novel way to represent the 32 crystallographic point

- groups," *J. Mater. Educ.*, vol. 20, **1999**.
- [13] M. A. Jaswon, *An Introduction to Mathematical Crystallography*. London: Longmans, **1965**.
- [14] P. G. Radaelli, "Crystal Structure and Dynamics Part 1: Symmetry in the solid state," **2015**.
- [15] D. Peck and E. Delventhal, "Hermann-Mauguin Symmetry Symbols." [Online]. Available: <https://www.mindat.org/article.php/2742/Hermann-Mauguin+Symmetry+Symbols>. [Accessed: 28-May-2019].
- [16] C. R. Hubbard and L. D. Calvert, "The pearson symbol," *Bull. Alloy Phase Diagrams*, vol. 2, no. 2, pp. 153–157, **1981**.
- [17] H. Wondratschek, "Introduction to Space-Group Symmetry," in *International Tables for Crystallography Volume A*, 5th ed., T. Hahn, Ed. Springer, **2005**.
- [18] T. Hahn and A. Looijenga-Vos, "Contents and Arrangement of the tables," in *International Tables for Crystallography Volume A*, 5th ed., T. Hahn, Ed. **2005**.
- [19] W. Massa, *Crystal structure determination*. Springer Science & Business Media, **2013**.
- [20] T. Hahn, Ed., "International Tables for Crystallography-Space Group 164," in *International Tables for Crystallography Volume A*, vol. A, Springer, pp. 540–541, **2006**.
- [21] R. Nikolova and V. Kostov-Kytin, "Crystal chemistry of 'glaserite' type compounds," *Bulg. Chem. Commun.*, vol. 45, no. 4, pp. 418–426, **2013**.
- [22] M. I. Aroyo, J. M. Perez-Mato, D. Orobengoa, E. Tasci, G. De La Flor, and A. Kirov, "Crystallography online: Bilbao crystallographic server," *Bulg. Chem. Commun*, vol. 43, no. 2, pp. 183–197, **2011**.
- [23] E. S. Tasci, G. de la Flor, D. Orobengoa, C. Capillas, J. M. Perez-Mato, and M. I. Aroyo, "An introduction to the tools hosted in the Bilbao Crystallographic Server," *EPJ Web Conf.*, vol. 22, p. 22, Mar. **2012**.
- [24] C. Capillas, J. M. Perez-Mato, and M. I. Aroyo, "Maximal symmetry transition paths for reconstructive phase transitions," *J. Phys. Condens. Matter*, vol. 19, no. 27, p. 275203, **2007**.
- [25] E. S. Tasci, G. De La Flor, and M. I. Aroyo, "Obtaining the transformation matrix connecting two group-subgroup related structures," in *IUCr Mieres:*

Crystallographic Computing School, August 16-22, 2011.

- [26] K. Momma and F. Izumi, "VESTA 3 for three-dimensional visualization of crystal, volumetric and morphology data," *J. Appl. Crystallogr.*, vol. 44, no. 6, pp. 1272–1276, **2011**.
- [27] S. Ivantchev, E. Kroumova, G. Madariaga, J. M. Pérez-Mato, and M. I. Aroyo, "*SUBGROUPGRAPH*: a computer program for analysis of group–subgroup relations between space groups," *J. Appl. Crystallogr.*, vol. 33, no. 4, pp. 1190–1191, Aug. **2000**.
- [28] J. W. Eaton, D. Bateman, S. Hauberg, and R. Wehbring, "GNU Octave version 5.1.0 manual: a high-level interactive language for numerical computations.," **2019**.
- [29] G. Flor, D. Orobengoa, E. Tasci, J. M. Perez-Mato, and M. I. Aroyo, "Comparison of structures applying the tools available at the Bilbao Crystallographic Server," *J. Appl. Crystallogr.*, vol. 49, no. 2, pp. 653–664, **2016**.
- [30] Hudson Institute of Mineralogy, "Aphthitalite." [Online]. Available: <https://www.mindat.org/min-280.html#autoanchor15>. [Accessed: 17-May-2019].
- [31] B. Gossner, "Über die Kristallstruktur von Glaserit und Kaliumsulfat," *Neues Jahrb. Miner. B.-Band*, vol. 57, pp. 89–116, **1928**.
- [32] P. B. Moore, "COMPLEX CRYSTAL-STRUCTURES RELATED TO GLASERITE, K₃Na(SO₄)₂-EVIDENCE FOR VERY DENSE PACKINGS AMONG OXYSALTS," *Bull. Mineral.*, vol. 104, no. 4, pp. 536–547, **1981**.
- [33] M. Mathew and S. Takagi, "Structures of biological minerals in dental research," *J. Res. Natl. Inst. Stand. Technol.*, vol. 106, no. 6, p. 1035, **2001**.
- [34] K. Okada and J. Oosaka, "Structures of potassium sodium sulphate and tripotassium sodium disulphate," *Acta Crystallogr. Sect. B Struct. Crystallogr. Cryst. Chem.*, vol. 36, no. 4, pp. 919–921, **1980**.
- [35] B. I. Lazoryak, "Design of inorganic compounds with tetrahedral anions," *Russ. Chem. Rev.*, vol. 65, no. 4, pp. 287–305, **1996**.
- [36] C. Calvo and R. Faggiani, "Crystal structure of the glaserite form of BaNaPO₄," *Can. J. Chem.*, vol. 53, no. 12, pp. 1849–1853, **1975**.
- [37] V. A. Morozov, B. I. Lazoryak, A. P. Malakho, K. V Pokholok, S. N.

- Polyakov, and T. P. Terekhina, "The Glaserite-like Structure of Double Sodium and Iron Phosphate $\text{Na}_3\text{Fe}(\text{PO}_4)_2$," *J. Solid State Chem.*, vol. 160, no. 2, pp. 377–381, **2001**.
- [38] D. Orobengoa, C. Capillas, M. I. Aroyo, J. M. Perez-Mato, and IUCr, "AMPLIMODES: symmetry-mode analysis on the Bilbao Crystallographic Server," *J. Appl. Crystallogr.*, vol. 42, no. 5, pp. 820–833, Oct. **2009**.
- [39] G. Bergerhoff, M. Berndt, K. Brandenburg, T. Degen, and IUCr, "Concerning inorganic crystal structure types," *Acta Crystallogr. Sect. B Struct. Sci.*, vol. 55, no. 2, pp. 147–156, Apr. **1999**.
- [40] C. Capillas, E. S. Tasci, G. de la Flor, D. Orobengoa, J. M. Perez-Mato, and M. I. Aroyo, "A new computer tool at the Bilbao Crystallographic Server to detect and characterize pseudosymmetry," *Zeitschrift für Krist.*, vol. 226, no. 2, pp. 186–196, Feb. **2011**.



HACETTEPE UNIVERSITY
GRADUATE SCHOOL OF SCIENCE AND ENGINEERING
THESIS/~~DISSERTATION~~ ORIGINALITY REPORT

HACETTEPE UNIVERSITY
GRADUATE SCHOOL OF SCIENCE AND ENGINEERING
TO THE DEPARTMENT OF PHYSICS ENGINEERING

Date: 11/07/2019

Thesis Title / ~~Topic~~: Classification of the Glaserite Structures Family by means of Group Theory / Grup Teorisi ile Glaserit Yapılar Ailesinin Sınıflandırılması

According to the originality report obtained by myself/my thesis advisor by using the Turnitin plagiarism detection software and by applying the filtering options stated below on 10/07/2019 for the total of 84 pages including the a) Title Page, b) Introduction, c) Main Chapters, d) Conclusion sections of my thesis entitled as above, the similarity index of my thesis is 9 %.

Filtering options applied:

1. Bibliography/Works Cited excluded
2. Quotes excluded /~~included~~
3. Match size up to 5 words excluded

I declare that I have carefully read Hacettepe University Graduate School of Science and Engineering Guidelines for Obtaining and Using Thesis Originality Reports; that according to the maximum similarity index values specified in the Guidelines, my thesis does not include any form of plagiarism; that in any future detection of possible infringement of the regulations I accept all legal responsibility; and that all the information I have provided is correct to the best of my knowledge.

I respectfully submit this for approval.

Date and Signature

11.07.2019

Name Surname: Serpil Albay

Student No: N12226679

Department: Physics Engineering

Program: Physics Engineering

Status: Masters Ph.D. Integrated Ph.D.

ADVISOR APPROVAL

APPROVED.

Assoc. Prof. Dr. Emre Taşçı

CURRICULUM VITAE

Name, Surname : Serpil Albay
e-mail : serpilalbay@gmail.com

Education

B.Sc. : Middle East Technical University, Faculty of Arts and Science, Physics (2006-2013)

M.Sc. : Hacettepe University, Graduate School of Science and Engineering, Physics Engineering (2013-2019)

Work Experiences

2016 - now : Turkish Anti-Doping Commission, Ankara, Turkey

- Freelance doping control officer in sport competitions at country-wide

2016 - 2017 : International Middle East Peace Research Center, Ankara, Turkey

- IT&Database Assistant for UNHCR Project

2016 : Nanomagnetism Instruments, Ankara, Turkey

- Sales of atomic force microscopy (AFM)

- 2013 - 2015 : V-Count Technology, Ankara, Turkey
- Configuration, calibration and testing of V-Count devices for abroad customer via remote connection sessions
- 2013 : Çankaya University, Ankara, Turkey
- Teaching assistant in Material Science and Engineering Department
- 2011 - 2019 : Lionbridge Company
- Freelance Internet Assessor of Google Search Engine